

## Synthesis of Anthranilyldoxime Derivatives as Estrogen Receptor Ligands and Computational Prediction of Binding Modes

Tiziano Tuccinardi,<sup>†</sup> Simone Bertini,<sup>†</sup> Adriano Martinelli,<sup>†</sup> Filippo Minutolo,<sup>\*,‡</sup> Gabriella Ortore,<sup>†</sup> Giorgio Placanica,<sup>†</sup> Giovanni Prota,<sup>†</sup> Simona Rapposelli,<sup>†</sup> Kathryn E. Carlson,<sup>‡</sup> John A. Katzenellenbogen,<sup>‡</sup> and Marco Macchia<sup>†</sup>

Dipartimento di Scienze Farmaceutiche, Università di Pisa, Via Bonanno 6, 56126 Pisa, Italy, and  
Department of Chemistry, University of Illinois, 600 S. Goodwin Avenue, Urbana, Illinois 61801

Received May 11, 2006

*N*-Me-anthranilyldoximes possess a hydrogen-bonded pseudocyclic A' ring in place of the typical phenolic A-ring that is characteristic of most estrogen receptor (ER) ligands. We have investigated the role played by substituents introduced into either one or both of the peripheral 3- and 4-phenyl rings in modulating ER binding affinity. An efficient synthetic strategy was employed for the preparation of differentially substituted 3- and 4-aryl derivatives that involved exploiting the different reactivity of bromo- versus chloro-aryl groups in palladium-catalyzed cross-couplings. The binding data showed that ER $\alpha$  affinity could be improved by a single *p*-OH group in the 4-phenyl ring, whereas the same substitution on the 3-phenyl ring caused a dramatic reduction of ER $\beta$  affinity. The most ER $\alpha$ -selective compound was the one with two *p*-OH groups on both phenyl substituents. To rationalize these results, ligand docking followed by molecular mechanics Poisson–Boltzmann/surface area (MM-PBSA) studies were carried out. These analyses suggested a molecular basis for the interaction of these compounds with the ERs and enabled the development of models able to predict the mode of ligand binding.

### Introduction

The actions of estrogens in many organs and tissues (reproductive, skeletal, cardiovascular, and central nervous) are mediated by estrogen receptors (ERs), which are members of a superfamily of nuclear receptors that function as ligand-activated gene transcription factors.<sup>1</sup> There are two subtypes of estrogen receptors known as ER $\alpha$  and ER $\beta$ ,<sup>2,3</sup> and they have a very high amino acid sequence identity in their DNA-binding domains (DBDs) but a more modest (59%) homology in their ligand-binding domains (LBDs).<sup>4</sup> Despite the sequence divergence in the LBD amino acid sequences, however, X-ray analyses of receptor–ligand complexes have shown that the binding cavities of ER $\alpha$  and ER $\beta$  are extremely similar. The differences are at two amino acid residues (ER $\beta$  has a methionine (M336) in place of the leucine at position 384 of ER $\alpha$  and an isoleucine (I373) instead of the methionine at position 421 of ER $\alpha$ ) and in the pocket volume (ER $\beta$  being somewhat smaller than ER $\alpha$ ).<sup>5,6</sup> The two receptor subtypes have quite different tissue distributions. In fact, ER $\alpha$  is more enriched in certain reproductive organs, such as the uterus and mammary glands, whereas ER $\beta$  is mostly expressed in other tissues, such as the central nervous system, colon, lung, prostate, and the urinary tract.<sup>7</sup>

Selective estrogen receptor modulators (SERMs)<sup>8</sup> are a special category of estrogens, mostly of a nonsteroidal nature, that show an estradiol agonist-like action in some tissues but antagonize estradiol in others. They are particularly attractive as therapeutic agents because they are able to block estrogen action at those sites where stimulation would be undesirable (i.e., breast and uterus), whereas at the same time, they stimulate estrogen actions in other tissues where they are desired, (i.e., the bone and liver).<sup>9,10</sup> The tissue-selective pharmacology of SERMs is probably due both to their different actions on each ER subtype

and/or by the different interactions that the ER–ligand complex might have with the cellular coregulatory proteins or effector components that vary from tissue to tissue and gene to gene.<sup>11,12</sup>

Our search for new ER ligands has initially led us to develop 3,4-diarylsalicyldoximes, either unsubstituted on the phenyl rings (**1a**)<sup>13</sup> or containing para hydroxy groups on either one (**1b,c**)<sup>14</sup> or on both (**1d**)<sup>14</sup> peripheral substituents. These compounds were particularly interesting because they contained an unprecedented bioisosteric replacement of the phenolic A group, which is a common feature of typical steroidal and nonsteroidal ER ligands.<sup>15</sup> In salicyldoximes **1a–d**, there is a six-membered pseudocycle A' formed by the intramolecular hydrogen bond between the phenolic OH and the adjacent oxime nitrogen atom, which might be functioning as an effective mimic of the phenolic A-ring.

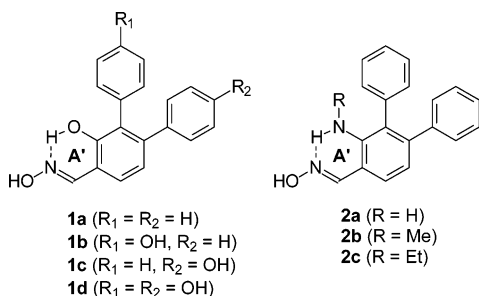
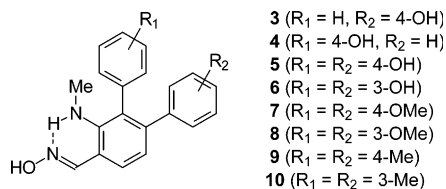
In binding assays, unsubstituted salicyldoxime **1a** proved to possess an interesting affinity for both receptor subtypes (relative binding affinity (RBA) = 1.13% with ER $\alpha$  and 1.71% with ER $\beta$ ; RBA (estradiol) = 100%). The binding properties were further improved with the introduction of a single *p*-OH group, whose position resulted in only a slight shift in the ER $\alpha$ /ER $\beta$  selectivity profile of **1b** and **1c**. As a matter of fact, when the *p*-OH is introduced in the proximal (position 3) aryl ring (**1b**), the affinity for the ER $\beta$  is increased (RBA = 2.21%), whereas when the same group is placed on the other (distal) aryl substituent (**1c**), the binding preference for ER $\alpha$  increases (RBA = 2.59%).<sup>14</sup> However, the simultaneous presence of two *p*-OH groups on both phenyl substituents (**1d**) caused a dramatic reduction in the binding affinities, especially in the case of ER $\beta$ .<sup>14</sup>

In a parallel study, we also wanted to further investigate the structural basis for the phenol mimicry of pseudocycle A' to see whether we could improve ER binding affinity by modifying the stereoelectronic nature of this ring. Therefore, we first synthesized anthranilyldoxime **2a**, in which the oxygen atom of salicyldoximes was replaced by an aniline-type nitrogen, and then, we also prepared anthranilyl derivatives possessing

\* Corresponding author. Tel: +39 050 2219557. Fax: +39 050 2219605.  
E-mail: minutolo@farm.unipi.it.

<sup>†</sup> Università di Pisa.

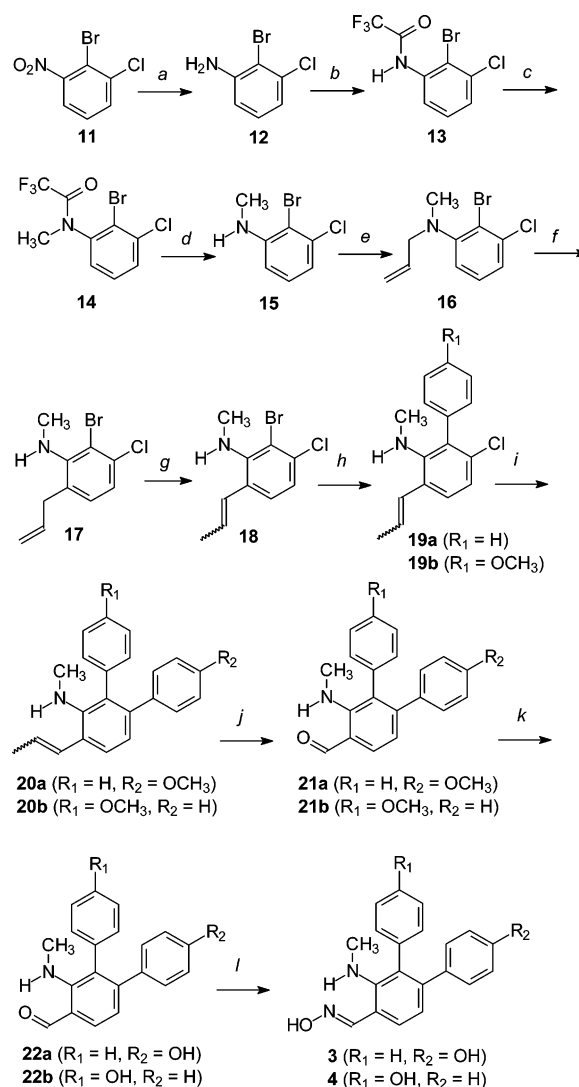
<sup>‡</sup> University of Illinois.

**Chart 1.** Estrogen Ligands Possessing Salicylaldoxime (**1a–d**) and Anthranlyaldoxime (**2a–c**) Structures**Chart 2.** Newly Synthesized *N*-Methylantranylaldoximes (**3–10**)

small alkyl groups on the nitrogen atom (a methyl in **2b** and an ethyl in **2c**) to see whether these groups would affect the binding properties of this class of molecules.<sup>16</sup> The *N*-unsubstituted derivative **2a** proved to possess better binding properties than its salicylic analogue **1a**, showing a 2-fold improvement in both receptor subtypes. A further increase was observed with *N*-methylated analogue **2b**, which showed RBA values three times higher than that of **1a** on both receptor subtypes. On the contrary, the *N*-ethylated derivative **2c** showed a very significant drop in binding properties compared to those of its *N*-methylated analogue **2b**, with a nearly 10-fold reduction on ER $\alpha$  and a remarkable over a 100-fold reduction on ER $\beta$ . These results could be explained by docking experiments which showed that the *N*-methyl group of **2b** is found to occupy a small hydrophobic pocket whose boundaries are formed by three residues (ER $\alpha$ : Leu346, Leu349, and Ala350). However, the spatial dimension of this pocket is only able to comfortably host the *N*-Me group of **2b** so that it needs to rearrange to be able to do the same with even the slightly bulkier ethyl moiety, as in **2c**; the resulting repulsive van der Waals interactions caused the decreased affinity.<sup>16</sup> Therefore, the best phenolic A-ring substitute found with our initial investigations was the pseudo-cycle A' of *N*-Me anthranlyaldoxime (**2b**).

On the basis of these considerations, we wanted to combine the beneficial effects of peripheral substituents of the salicylaldoxime series with the highest affinity pseudocycle A' represented by the *N*-Me anthranlyaldoxime (**2b**). Therefore, in this article, we expanded the series of *N*-Me anthranlyaldoximes by introducing various substituents on the 3- and 4-phenyl rings of **2b**. Heterodisubstituted compounds **3** and **4** are characterized by the presence of a *para* hydroxy group on either one of the aryl substituents, in parallel to what was previously designed in the salicylaldoxime series with compounds **1c** and **1b**, respectively. In the homodisubstituted series (compounds **5–10**), we wanted to verify the effect on binding affinity caused by the presence of polar (OH, OMe) or hydrophobic (Me) substituents in *meta* and *para* positions of both peripheral aryl rings.

To investigate the molecular interactions that are important in determining the affinity of these ligands toward the ERs and also to clarify the spatial orientations that all of the anthranlyaldoxime series assume within the receptors, various compu-

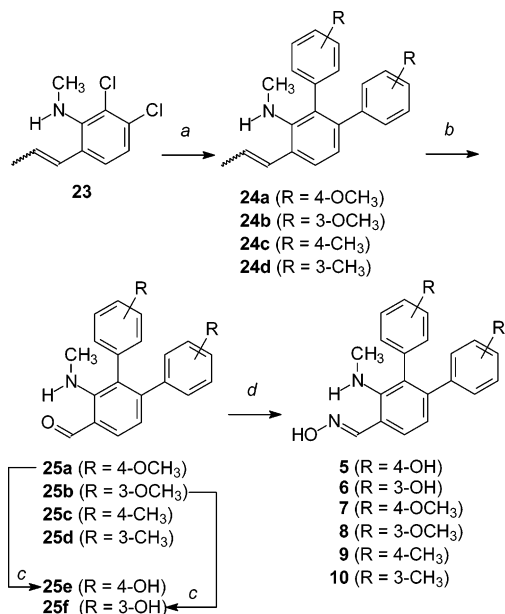
**Scheme 1**<sup>a</sup>

<sup>a</sup> Key: (a)  $NH_2NH_2 \cdot H_2O$ ,  $FeCl_3 \cdot 6H_2O$ , activated carbon, MeOH,  $\Delta$ ; (b)  $(CF_3CO)_2O$ ,  $K_2CO_3$ , acetone; (c) MeI,  $K_2CO_3$ , DMF; (d)  $K_2CO_3$ ,  $H_2O$ /MeOH; (e) allyl bromide,  $K_2CO_3$ , acetonitrile, 80 °C; (f)  $BF_3 \cdot Et_2O$ , sulfolane, 120 °C; (g) *t*-BuOK, DMSO, RT; (h)  $4-R_1-C_6H_4B(OH)_2$ ,  $Pd(PPh_3)_4$ ,  $Na_2CO_3$ , toluene, EtOH,  $\Delta$ ; (i)  $4-R_2-C_6H_4B(OH)_2$ ,  $Pd_2(dba)_3$ ,  $Cy_3P$ ,  $Cs_2CO_3$ , dioxane,  $\Delta$ ; (j)  $OsO_4$ , NaIO<sub>4</sub>, dioxane-H<sub>2</sub>O; (k)  $BBr_3$ ,  $CH_2Cl_2$ ,  $-78 \rightarrow 0$  °C; (l)  $NH_2OH \cdot HCl$ , MeOH-H<sub>2</sub>O, 50 °C.

tational models of ER $\alpha$  and ER $\beta$  were developed. Previously reported anthranlyaldoximes **2a–c**<sup>16</sup> and newly synthesized compounds **3–10** were subjected to an automated docking molecular dynamics (MD) simulation protocol followed by a molecular mechanics Poisson–Boltzmann/surface area (MM-PBSA) analysis,<sup>17</sup> and quantitative relationships between the experimental and calculated free energy of binding were evaluated with the aim to develop a predictive model.

## Results and Discussion

**Synthetic Chemistry.** The preparation of heterodisubstituted compounds **3** and **4** (Scheme 1) included key steps we had already developed,<sup>14</sup> represented by a sequential double Pd-catalyzed cross-coupling reaction on a bromo-chloro-disubstituted aryl precursor. This approach exploits the different reactivities of aryl-bromides and aryl-chlorides toward boronic acids under different reaction conditions, that is, Suzuki-type conditions for the bromides<sup>18</sup> and Fu-type conditions for the chlorides,<sup>19</sup> and it provides an efficient way to selectively

Scheme 2<sup>a</sup>

<sup>a</sup> Key: (a) 2 times: Pd<sub>2</sub>(dba)<sub>3</sub>, Cy<sub>3</sub>P, ArB(OH)<sub>2</sub>, Cs<sub>2</sub>CO<sub>3</sub>, dioxane, 80 °C; (b) OsO<sub>4</sub>, NaIO<sub>4</sub>, dioxane-H<sub>2</sub>O; (c) BBr<sub>3</sub>, CH<sub>2</sub>Cl<sub>2</sub>, -78 → 0 °C; (d) NH<sub>2</sub>OH·HCl, MeOH-H<sub>2</sub>O, 50 °C.

introduce different substituents in those positions, depending on the boronic acid used. The complete synthesis of **3** and **4** was accomplished as shown in Scheme 1.

2-Bromo-3-chloronitrobenzene (**11**)<sup>20</sup> was first reduced with hydrazine hydrate in the presence of catalytic amounts of ferric chloride and activated carbon to yield the corresponding aniline **12**. Treatment with trifluoroacetic anhydride afforded trifluoroacetamide **13**, which was methylated with MeI to give tertiary amide **14**. Alkaline hydrolysis afforded *N*-methylamine **15**, which underwent an *N*-allylation reaction with allyl bromide. *N*-Allyl-*N*-methylaniline (**16**) was submitted to an aza-Claisen rearrangement in the presence of boron trifluoride etherate, which selectively gave *ortho*-allylated aniline **17**. The alkaline rearrangement of the terminal double bond to the internal position afforded styrene derivative **18** as an *E/Z* diastereomeric mixture.

At this point, the bromo-chloro substituted intermediate **18** was first submitted to a classical Suzuki-type cross-coupling reaction, using Pd(PPh<sub>3</sub>)<sub>4</sub> as the catalyst, to introduce the first phenyl or *p*-methoxyphenyl group in place of the bromine atom, affording compounds **19a** (R<sub>1</sub> = H) or **19b** (R<sub>1</sub> = OCH<sub>3</sub>), respectively. This step did not affect the chlorine atom of **18**, which was then substituted in the second cross-coupling reaction with *p*-methoxyphenyl or unsubstituted phenyl boronic acid, using the more reactive catalytic system comprised of Pd<sub>2</sub>(dba)<sub>3</sub>, together with tricyclohexylphosphine as the catalyst ligand. Under these conditions, it was possible to introduce a second aryl substituent (R<sub>2</sub> = OCH<sub>3</sub> for **20a**; R<sub>2</sub> = H for **20b**) in place of the aryl-chloride groups of **19a** and **19b**.

Salicylaldehydes **21a,b** were then obtained by oxidative cleavage of the double bond of **20a,b**, using sodium periodate in the presence of catalytic amounts of osmium tetroxide. The transformation of the methoxy groups of **21a,b** into hydroxyls was achieved by a BBr<sub>3</sub> demethylation, and the resulting hydroxyaryl-substituted salicylaldehydes **22a,b** were then condensed with hydroxylamine hydrochloride in a methanol-water mixture at 50 °C to give final oximes **3** and **4**.

The synthesis of homodisubstituted oximes **5–10** is shown in Scheme 2.

Table 1. Relative Binding Affinities<sup>a</sup> of Compounds **2–10** for Estrogen Receptors α and β

ligand	hERα	hERβ
estradiol	(100)	(100)
<b>2b</b> <sup>b</sup>	3.7 ± 1.1 <sup>b</sup>	5.2 ± 1.2 <sup>b</sup>
<b>3</b>	5.38 ± 1.37	1.11 ± 0.01
<b>4</b>	1.17 ± 0.33	0.72 ± 0.10
<b>5</b>	1.96 ± 0.54	0.14 ± 0.04
<b>6</b>	0.14 ± 0.03	0.05 ± 0.01
<b>7</b>	2.33 ± 0.20	0.47 ± 0.14
<b>8</b>	0.65 ± 0.19	0.14 ± 0.03
<b>9</b>	0.95 ± 0.07	1.86 ± 0.26
<b>10</b>	3.91 ± 0.30	2.13 ± 0.56

<sup>a</sup> Determined by a competitive radiometric binding assay with [<sup>3</sup>H]estradiol; preparations of purified, full-length human ERα and ERβ (PanVera) were used (see Experimental Section). The values are reported as the mean ± SD of three independent experiments; the K<sub>d</sub> for estradiol for ERα is 0.2 nM and for ERβ is 0.5 nM. <sup>b</sup> See ref 16.

(*E,Z*)-2,3-Dichloro-*N*-methyl-6-(1-propenyl)aniline (**23**), obtained as previously reported,<sup>16</sup> underwent a double cross-coupling reaction with the appropriate arylboronic acid, using the catalytic system containing Pd<sub>2</sub>(dba)<sub>3</sub> and tricyclohexylphosphine, which efficiently promotes cross-coupling reactions on aryl-chloride bonds. Under these conditions, diaryl-substituted products **24a–d** were obtained. Anthranilylaldehydes **25a–d** were then obtained by oxidative cleavage of the double bond of **14a–c**, using sodium periodate in the presence of catalytic amounts of osmium tetroxide. Hydroxy-substituted aldehydes **24e,f** were obtained by the demethylation of **25a,b**, respectively, with BBr<sub>3</sub>. The final condensation of aldehydes **25a–f** with hydroxylamine hydrochloride in a 10:1 methanol-water mixture at 50 °C yielded *N*-methylanthranilyldoximes **5–10**.

In all cases (**3–10**), the (*E*)-form of the oxime was the only diastereoisomer formed, presumably because the intramolecular hydrogen bond, which can only form in the (*E*)-isomer, contributes to the oxime stability. As seen before for similar compounds,<sup>13,14,16</sup> in these cases, the chemical shift value of the oxime proton, which is always found below 8 ppm (8.33 for **7**; 8.34 for **5**; 8.35 for **6**; 8.36 for **3**, **4**, **8**, and **9**; 8.37 for **10**), confirmed the (*E*)-configuration of oximes **5–10**.<sup>21</sup>

**Estrogen Receptor Binding Assays.** The binding affinity of oximes **3–10** for both ERα and ERβ were determined by a radiometric competitive binding assay, using methods that have been described elsewhere in detail.<sup>22,23</sup> In Table 1, the RBA values for the newly reported compounds, determined with purified full-length human alpha (hERα) and beta (hERβ) receptor subtypes, together with those previously obtained for **2b** are reported.<sup>16</sup> Binding affinity (RBA) values are reported relative to that of estradiol (E<sub>2</sub>), which is set at 100%.

The results shown in Table 1 indicate that the anthranilyldoxime bearing a single para hydroxy group in the distal aryl ring, that is, compound **3**, experiences an increase in its binding affinity for ERα (RBA = 5.38%) compared with unsubstituted **2b**, whereas its affinity for ERβ is significantly reduced (RBA = 1.11%). The affinity for ERα found with **3** is the highest ever found with our pseudocycle-phenol mimics derivatives,<sup>13,14,16</sup> corresponding to a K<sub>d</sub> of 3.7 nM. A similar increased ERα/ERβ selectivity ratio caused by the introduction of a *p*-OH into the distal phenyl substituent had already been observed in the salicylaldoxime series (**1c**),<sup>14</sup> although to a lesser extent. However, when the same *para* hydroxy group is placed on the other aryl ring (proximal) as in **4**, the affinity decreases with both receptor subtypes. This time, no parallelism with the salicylaldoxime series was found because in that series the same

structural modification (*p*-OH on the proximal ring, as in **1b**) had caused a significant shift in affinity toward ER $\beta$  selectivity.

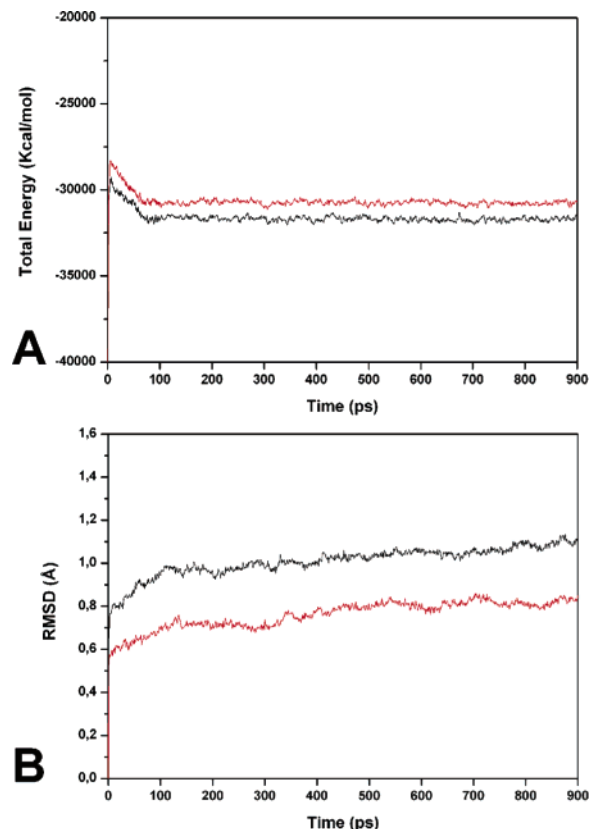
Among the homodisubstituted compounds, the 4-OH disubstituted oxime **5** shows a dramatic drop in its affinity for ER $\beta$ , although still preserving a good binding ability on ER $\alpha$ , with an  $\alpha/\beta$  selectivity  $K_d$  ratio of 36. Oxime **7**, possessing two *para*-methoxy substituents, confirms the general trend observed for its nonmethylated counterpart **5**, with a comparable affinity for ER $\alpha$  but a lower degree of  $\alpha/\beta$  selectivity due to a slight raise of ER $\beta$  affinity. The binding properties of oximes **6** and **8**, which have the oxygenated substituents (OH and OMe, respectively) in the *meta* positions of both peripheral aromatic groups, are low on both receptor subtypes. These results indicate that the introduction of two oxygenated substituents, such as OMe and OH, generally result in a reduction in ER $\beta$  affinity. ER $\alpha$  affinity is only slightly affected when these substituents are placed in the two *para* positions, whereas their introduction into the *meta* positions is not tolerated by either of the two receptor subtypes. Compound **9**, having two *para*-methyl groups, has an affinity for ER $\beta$ , which is twice as high as for ER $\alpha$ . In contrast, analogue **10**, where the methyl groups are placed on the *meta* positions, has a preference for ER $\alpha$  (RBA = 3.91%) rather than ER $\beta$ . An interesting profile is found with the introduction of this small lipophilic substituent (Me) in the *para*- (**10**) and *meta* positions (**9**) of the two aryl rings. In fact, in one case (*para*-methyl, **9**), the RBA ER $\beta$ /ER $\alpha$  ratio is about 2, whereas when the methyl is shifted to the *meta* position (**10**), the RBA alpha/beta ratio is completely reversed (ER $\alpha$ /ER $\beta$   $\approx$  2).

**Docking Analysis.** A series of docking simulations have been carried out to better rationalize the experimental binding affinities of the whole series of anthranyldoximes, including the previously reported (**2a–c**)<sup>16</sup> and the newly synthesized (**3–10**) compounds. To build the receptor models, X-ray structures of ER $\alpha$  (1G50<sup>24</sup>) and ER $\beta$  (1X7J<sup>25</sup>) were complexed with estradiol, and the complexes were subjected to 900 ps of molecular dynamics (MD) simulations (see Experimental Section for details). As shown in Figure 1A, after about 100 ps of MD, both systems reached an equilibrium because the total energy for the last 800 ps remained constant. Analyzing the root-mean-square deviation (RMSD) from the X-ray structures of all of the heavy atoms of the proteins, we observed that after an initial increase during the last 800 ps, the RMSD remained approximately constant, around the range of 0.9–1.0 Å for ER $\alpha$  and 0.7–0.8 Å for ER $\beta$  (Figure 1B).

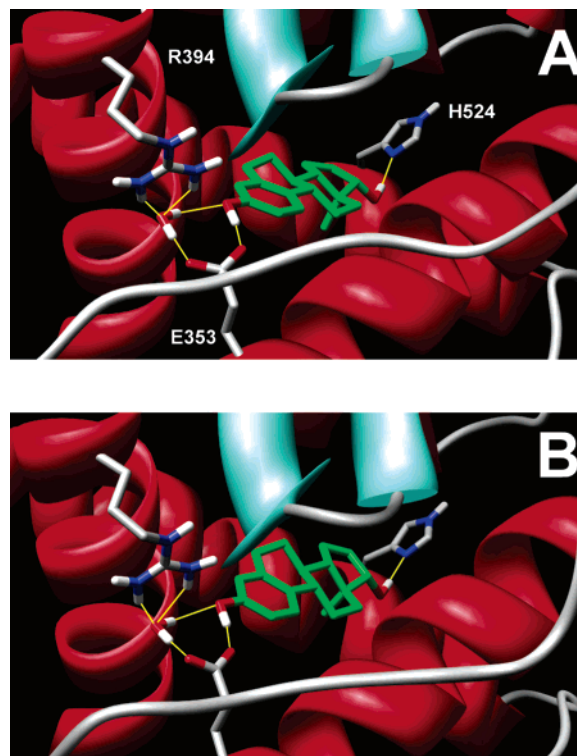
Figure 2 shows the minimized average structures of the binding site of the two receptors complexed with estradiol. As also confirmed by the H-bond analysis of the MD simulations (Table 2), estradiol presented a very similar interaction scheme into both receptors: the 17-hydroxy group interacted with H524-(475), and the 3-hydroxy substituent formed a H bond with E353(305) (residue numbers are given for both ER $\alpha$  and ER $\beta$ , the latter in parentheses). Furthermore, as already suggested by Brzozowski and Pike,<sup>26,27</sup> a water molecule is also present at the core of a H-bond network system between E353(305), R394-(346), and the 3-hydroxy substituent of estradiol.

Using the two minimized average structures reported above as receptors, the compounds showed in Table 1 were docked using an automated docking procedure by means of AUTODOCK 3.0<sup>28</sup> (see Experimental Section).

A conformational search of these ligands revealed the presence of an intramolecular H bond with the formation of a pseudocycle involving the oxime nitrogen and the *ortho* disposed N–H group. The quantum mechanics optimization of **2b** suggested that this interaction has a good strength, about 4 kcal/



**Figure 1.** Analysis of the MD simulation of estradiol complexed with ER $\alpha$  (black) and ER $\beta$  (red). (A) Total energy of the system (kcal/mol) vs time is reported; (B) RMSD between all of the heavy atoms of the receptors and the two X-ray starting structures is reported.

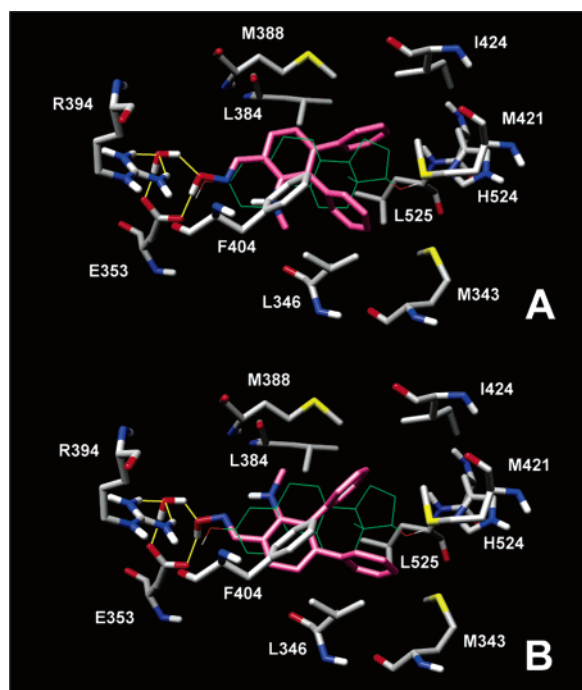


**Figure 2.** Hydrogen-bonding network of the estradiol in the ER $\alpha$  (panel A) and ER $\beta$  (panel B).

mol (see Experimental Section for details), and consequently, this H bond was maintained during interaction in the binding site. For this reason, during the AUTODOCK protocol, we

**Table 2.** Hydrogen Bonds Analysis of the E353(305)–R394(346)–Water–Estradiol–H524(475) System during the MD Simulation into Both Receptor Subtypes

donor	acceptor <sub>h</sub>	acceptor	distance (Å)	% occupied
ER $\alpha$				
E353@OE2	EST@HO3	EST@O3	2.55	100
H524@ND1	EST@OH1	EST@O17	3.03	97
WAT@O	R394@HH12	R394@NH1	2.98	94.95
E353@OE1	WAT@H1	WAT@O	2.70	91.20
EST@O3	WAT@H2	WAT@O	2.95	65.75
WAT@O	R394@HH22	R394@NH2	3.24	63.10
ER $\beta$				
E305@OE2	EST@HO3	EST@O3	2.60	100
H475@ND1	EST@OH1	EST@O17	3.08	94.20
WAT@O	R346@HH12	R346@NH1	2.99	95.20
E305@OE1	WAT@H1	WAT@O	2.79	84.25
EST@O3	WAT@H2	WAT@O	3.1	59.21
WAT@O	R346@HH22	R346@NH2	3.18	70.80

**Figure 3.** Docking of compound **2b** into ER $\alpha$ . (A) Binding mode A; (B) binding mode B.

blocked the torsions involved in this intramolecular bond to prevent the loss of this interaction.

The docking studies revealed that as already hypothesized for other ER ligands<sup>29</sup> these compounds could interact with ERs through two different binding orientations as shown in Figure 3; these are designated as binding orientations A and B. In both cases, the hydrogen bonded pseudocycle present in **2b** mimicked the phenolic ring of estradiol, interacting with the E353(305)–R394(346)–H<sub>2</sub>O system. The same behavior was found for all of the other docked *N*-Me-anthranilyldoximes.

Concerning the other parts of the ligands in binding orientation A, the distal aromatic ring was directed toward H524(475) and interacted with L/M384(336), M388(340), M/I421(373), I424(376), and L525(476), whereas the proximal aromatic ring interacted with L346(298), F404(356), and M343(295). However, in binding orientation B, the distal aryl substituent interacted with L346(298), F404(356), and M343(295), whereas the proximal ring interacted with M388(340), L/M384(336), I424(376), and L525(476).

**Table 3.** Preferred Binding Orientation (pref.) of the Ligands into ER $\alpha$  and ER $\beta$ <sup>a</sup>

compd	ER $\alpha$		ER $\beta$	
	pref.	$\Delta E_{A-B}$	pref.	$\Delta E_{A-B}$
<b>2a</b>	A	--	A	-0.26
<b>2b</b>	A	-0.39	B	+0.37
<b>2c</b>	A	--	B	+0.48
<b>3</b>	A	-2.00	A	-0.44
<b>4</b>	A	-1.44	A	-0.37
<b>5</b>	A	--	A	-0.47
<b>6</b>	A	--	B	+0.15
<b>7</b>	A	-0.99	B	+0.49
<b>8</b>	A	--	B	+0.91
<b>9</b>	A	--	A	-0.85
<b>10</b>	A	-0.66	B	+0.31

<sup>a</sup> The free energy difference between orientation A and B, calculated by means of the AUTODOCK scoring function is also reported ( $\Delta E_{A-B}$ ). When AUTODOCK found only one of the two orientations, the free energy difference is indicated by "--".

As reported by Yang et al. for oxime derivatives,<sup>30</sup> there could be another possible orientation for aldoxime **3** (180° horizontal), in which the pseudocycle of the ligands interacted with H524(475), whereas the two aromatic rings were oriented toward the E353(305)–R394(346)–H<sub>2</sub>O system. This orientation was not taken into account because it was showed only by compound **9** inside the ER $\alpha$  and compound **2b** inside the ER $\beta$ . Furthermore, this alternative orientation was found to be energetically less stable than A and B orientations in both cases.

As shown in Table 3, in ER $\alpha$ , all of the ligands preferred orientation A, whereas in ER $\beta$ , six ligands preferred binding orientation B. However, for compound **2b** in ER $\alpha$  and compounds **2a–c**, **3–7**, and **10** in ER $\beta$ , the difference between the estimated free energy of binding for the two orientations was lower than 0.5 kcal/mol. Thus, although the AUTODOCK results could be considered reliable for indicating the preferred orientation for ER $\alpha$ , this was not the case for ER $\beta$ .

Six compounds out of 11 (**2a**, **2c**, **5**, **6**, **8**, and **9**) did not show the B orientation inside the ER $\alpha$ , and this fact was somewhat surprising because the ER $\alpha$  binding site was very similar to that of ER $\beta$ . However, the docking analysis for these compounds revealed that orientation A inside the ER $\alpha$  binding site was very stable because the corresponding cluster was highly populated (more than 50% of the total runs).

As a further analysis, we also docked these six compounds inside the ER $\alpha$  by means of 250 runs instead of 100 runs. Nevertheless, even in this case, the B orientation was not found.

Therefore, to make a more precise analysis of the ligand–receptor interaction and to find more reliable results about the preferred orientation of the ligand into ER $\alpha$  and ER $\beta$ , all of the ligand–receptor complexes were used as starting structures for 500 ps of MD simulation.

Successively, the MD trajectories were further analyzed through the MM-PBSA method,<sup>17</sup> which has shown to accurately estimate the ligand–receptor energy interaction.<sup>31–33</sup> This approach averages contributions of gas-phase energies, solvation free energies, and solute entropies calculated for snapshots of the complex molecule as well as the unbound components extracted from MD trajectories according to the procedure fully described in the Experimental Section. In particular, for each ligand, we took into account as starting points both A and B orientations found by AUTODOCK in both ERs for a total of 44 calculations; in the case of the ligands for which AUTODOCK did not find any B orientation into the ER $\alpha$ , these structures were built on the basis of the B orientation found for unsubstituted compound **2b**.

In the Table reported in the Supporting Information, the MM-PBSA results calculated for each ligand (A and B conformation) into both receptors are reported. The analysis of the energies differences between the two orientations for each ligand highlighted that all of the compounds showed the A orientation as the preferred one in both receptors; only the **5**-ER $\beta$  complex showed a better interaction energy when compound **5** was positioned into the B orientation. Interestingly, this compound was the one with the highest ER $\alpha$ /ER $\beta$  selectivity.

After the MD simulations, the ligand interactions observed in the starting structures (obtained by means of AUTODOCK) were generally maintained. In both orientations, the oxime hydroxy group interacted with the E353(305)-R394(346)-H<sub>2</sub>O system, whereas the two aromatic groups interacted with M343(295), L346(298), L/M384(336), M388(340), F404(356), M/I421(373), I424(376), and L525(476), as described above.

All of the compounds tested showed an affinity selectivity for ER $\alpha$ , and as already mentioned above, the ER $\alpha$  and ER $\beta$  binding sites are composed of identical residues except for the presence of L384 and M421 in ER $\alpha$ , which are substituted by M336 and I373 in ER $\beta$ . Moreover, the ER $\beta$  binding cavity is smaller than that of ER $\alpha$ , and this reduction is primarily due to the replacement of leucine at position 336 in ER $\alpha$  with the slightly bulkier methionine in ER $\beta$ .

In our receptor models, the compounds showed a lipophilic interaction with the methyl group of M421 in ER $\alpha$  and with the side chain of I373 in ER $\beta$ ; these interactions seemed to be stronger in ER $\alpha$  than in ER $\beta$ . As a matter of fact, for all of the tested ligands, the distance between the aromatic ring and the methyl group of M421 in ER $\alpha$  was about 3.4 Å; however, in ER $\beta$ , the distance between I373 and the same aromatic ring was always greater than 4 Å.

As for residue L/M384(336), it was far away from all of the ligands in both receptor subtypes (the distance was greater than 4 Å), and thus, the nature of the residue at this site appears to only slightly affect the ligand-receptor interaction.

In conclusion, it appears that the interaction of these ligands with the non conserved residue M421 in the ER $\alpha$  could be one of the reasons for their ER $\alpha$  selectivity. As examples of high- and low-affinity ligands, a binding interaction analysis of compounds **3** and **6** has been reported below.

Figure 4A shows the superposition of the binding sites of ER $\alpha$  and ER $\beta$  complexed with compound **3**, with the two nonconserved residues L/M384(336) and M/I421(373) represented as sticks. The compound formed H bonds with the E353(305)-R394(346)-H<sub>2</sub>O system through the oxime OH into both receptors; furthermore, the *para*-OH substituent formed a H bond with H524(475), simulating the interaction of the 17-hydroxy group of estradiol.

The H-bond interaction between the *para*-OH substituent and H475 in ER $\beta$  seems to be in contrast to the lower affinity of this compound, compared with that of the unsubstituted **2b**. The qualitative analysis is also confirmed by the quantitative one because the MM-PBSA procedure for ER $\beta$  calculated a greater affinity for compound **3** with respect to that for compound **2b** (Table 4). Thus, the computational procedures herein used, which are based on automated docking, the MD simulation, and the MM-PBSA analysis, seem to be unable to properly rationalize the affinity of compound **3** inside the ER $\beta$ .

The substitution of the *meta* position of each one of the two aromatic rings with a hydroxy group, as in **6**, resulted in a decrease in affinity with both receptors; Figure 4B shows the superposition of the binding sites of ER $\alpha$  and ER $\beta$  complexed with **6**, which was the lowest affinity compound with both

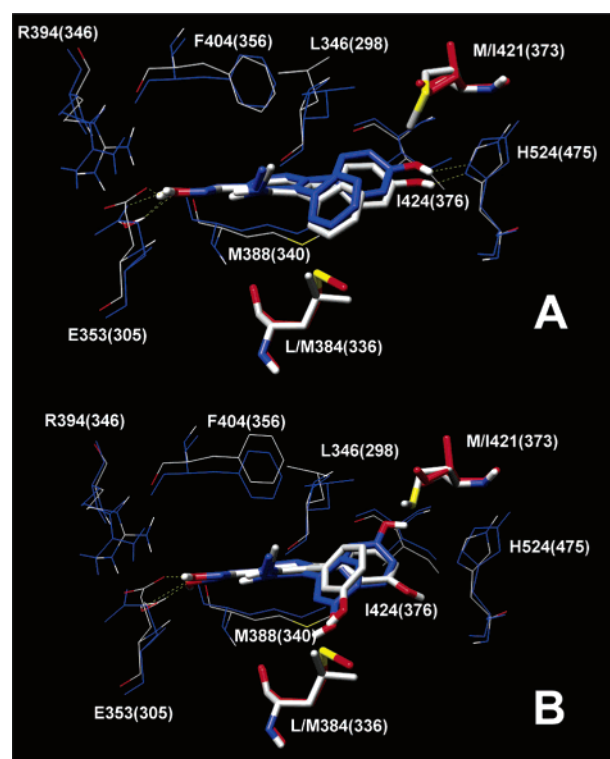


**Figure 4.** Superposition of the binding sites of ER $\alpha$  and ER $\beta$  complexed with compound **3** (panel A) and compound **6** (panel B). The ligand-ER $\alpha$  complex was colored by atom, whereas ligand-ER $\beta$  is in blue. The two nonconserved residues L/M384(336) and M/I421(373) (colored red in the ER $\beta$ ) are shown in stick representation.

**Table 4.** Energy Contributions to the Free Energy of Binding ( $\Delta G_{\text{cal}}$ , Expressed as kcal/mol) for the Best Ligand Orientation of Each Compound<sup>a</sup>

compd	ER $\alpha$					
	$\Delta E_{\text{MM}}$	$\Delta G_{\text{PBSA}}$	$-T\Delta S$	$\Delta G_{\text{cal}}$	$\Delta G_{\text{exp}}$	$\Delta\Delta G$
<b>2a</b>	-61.10	32.33	18.50	-10.27	-11.11	0.84
<b>2b</b>	-58.35	28.22	19.39	-10.74	-11.42	0.68
<b>2c</b>	-62.18	29.22	24.27	-8.69	-10.19	1.5
<b>3</b>	-65.85	35.35	19.26	-11.24	-11.64	0.40
<b>4</b>	-61.62	33.40	19.37	-8.85	-10.73	1.88
<b>5</b>	-70.53	37.31	22.74	-10.48	-11.04	0.56
<b>6</b>	-67.49	39.08	21.5	-6.91	-9.48	2.57
<b>7</b>	-69.84	36.80	22.44	-10.60	-11.14	0.54
<b>8</b>	-67.61	32.13	22.85	-12.63	-10.39	-2.24
<b>9</b>	-63.85	28.22	24.91	-10.72	-10.61	-0.11
<b>10</b>	-65.77	30.76	24.26	-10.75	-11.45	0.70
compd	ER $\beta$					
	$\Delta E_{\text{MM}}$	$\Delta G_{\text{PBSA}}$	$-T\Delta S$	$\Delta G_{\text{cal}}$	$\Delta G_{\text{exp}}$	$\Delta\Delta G$
<b>2a</b>	-58.72	30.50	17.5	-10.72	-10.61	-0.11
<b>2b</b>	-57.55	26.86	19.94	-10.75	-10.98	0.23
<b>2c</b>	-57.84	26.37	23.15	-8.32	-8.20	-0.12
<b>3</b>	-64.40	33.00	20.19	-11.21	-10.06	-1.15
<b>4</b>	-58.89	30.46	18.92	-9.51	-9.81	0.30
<b>5</b>	-83.21	53.66	20.58	-8.97	-8.85	-0.12
<b>6</b>	-67.63	40.97	19.96	-6.70	-8.18	1.48
<b>7</b>	-67.79	33.15	24.50	-10.14	-9.56	-0.58
<b>8</b>	-66.07	30.07	22.53	-13.47	-8.85	-4.62
<b>9</b>	-60.06	26.60	22.38	-11.08	-10.37	-0.71
<b>10</b>	-58.67	27.51	20.31	-10.85	-10.45	-0.40

<sup>a</sup> The energy difference ( $\Delta\Delta G$ ) between the calculated ( $\Delta G_{\text{cal}}$ ) and the experimental free energy of binding ( $\Delta G_{\text{exp}}$ ) is also reported.

receptors among all of the compounds tested. The Figure highlights that both *meta*-hydroxy substituents were unable to interact with any residue, confirming the binding affinity results.

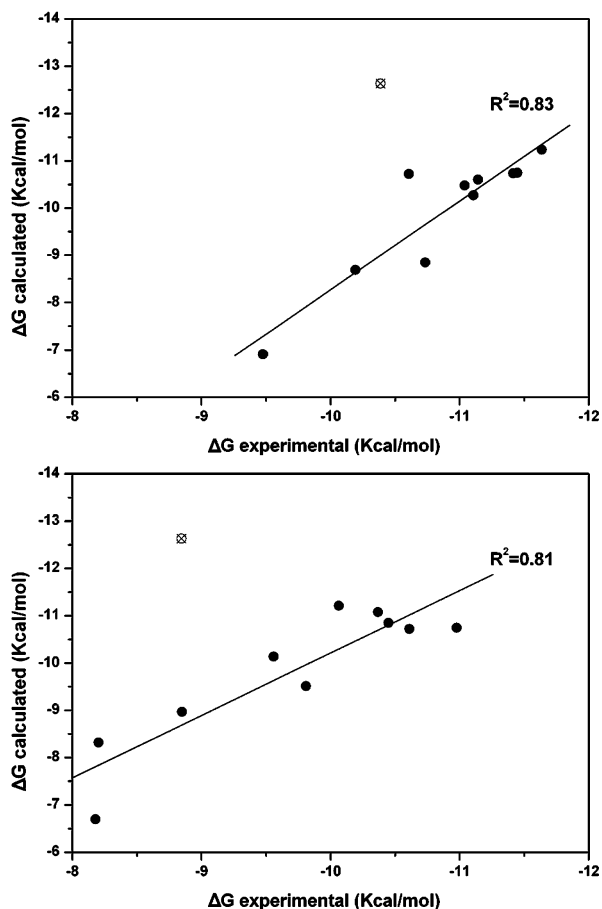


**Figure 5.** Experimental vs predicted free energy of binding for the eight ligands with ER $\alpha$  (upper) and ER $\beta$  (lower). The values are expressed as kcal/mol.

To verify whether the MM-PBSA method could be used to extrapolate a quantitative correlation between the calculated free energy and the experimental affinity of the ligands for ERs, we used the AMBER module *nmode* (see Experimental Section for details) to estimate the entropic contribution for the best 11 ligand–receptor complexes. As shown in Figure 5, a plot of the experimental versus the calculated free energy of binding (Table 4), considering compound **8** as an outlier, shows that there is a good quadratic correlation for both receptor subtypes ( $R^2 = 0.83$  for ER $\alpha$  and  $R^2 = 0.81$  for ER $\beta$ ).

With regard to compound **8**, the MM-PBSA method predicted a high affinity into both receptors, and as shown in the Table reported in the Supporting Information, these affinity values were mainly due to the van der Waals contribution, which was the highest one for both receptors. Although it was not possible to exclude the failure of the MM-PBSA approach for this outlier, it should be considered that the *meta*-methoxy group on both aromatic rings determined an increase of the hindrance of the ligand, and therefore, the low affinity of compound **8** could be due to a higher difficulty in reaching the binding site of both receptors.

## Conclusions

In conclusion, we expanded the series of *N*-Me anthranlyldoximes by introducing various substituents on the 3- and 4-phenyl rings of **2b**, combining the beneficial effects of the peripheral substituents of the salicyldoxime series (**1a–d**), with the highest affinity pseudocycle *A'* represented by the *N*-Me anthranlyldoxime nucleus. The synthetic strategy followed for

the preparation of compounds bearing different 3- and 4-aryl substituents (**3** and **4**) is particularly attractive because it exploits the differential reactivity of bromo- and chloro-aryl functionalities toward Pd-catalyzed cross-coupling reactions. The assays of binding affinities revealed that compound **3** has the highest affinity for ER $\alpha$  of our oxime series, with an RBA value of 5.38% ( $K_d$  of 3.7 nM) compared to that of E<sub>2</sub> ( $K_d$  of 0.2 nM), together with an ER $\alpha$ /ER $\beta$  selectivity  $K_d$  ratio of 12. Moreover, compound **5**, possessing two *p*-hydroxyphenyl substituents in the **3** and **4** positions, was the most ER $\alpha$  selective compound with an ER $\alpha$ /ER $\beta$  selectivity  $K_d$ -ratio of 36. Docking studies confirmed that in the whole series of anthranlyldoximes the oxime hydroxy group formed H bonds with the E353(305)–R394(346)–H<sub>2</sub>O system, mimicking the phenolic OH group of estradiol, and all of the compounds tested interacted in the ER $\alpha$  with the nonconserved residue M421, consistent with their ER $\alpha$ /ER $\beta$  selectivity. Furthermore, we reported calculations of binding free energies between these ligands and both ERs using the recently developed MM-PBSA method. This approach proved to be attractive for rationalizing in a quantitative manner the interaction of the anthranlyldoxime derivatives with ERs.

## Experimental Section

**Chemistry.** The melting points were determined on a Kofler hot-stage apparatus and are uncorrected. NMR spectra were obtained with a Varian Gemini 200 MHz spectrometer. Chemical shifts ( $\delta$ ) are reported in parts per million downfield from tetramethylsilane and referenced from solvent references. Electron impact (EI, 70 eV) mass spectra were obtained on an HP-5988A mass spectrometer. Where indicated, the elemental compositions of the compounds agreed to within  $\pm 0.4\%$  of the calculated value. Chromatographic separations were performed on silica gel columns by flash (Kieselgel 40, 0.040–0.063 mm; Merck) or gravity column (Kieselgel 60, 0.063–0.200 mm; Merck) chromatography. The reactions were followed by thin-layer chromatography (TLC) on Merck aluminum silica gel (60 F<sub>254</sub>) sheets that were visualized under a UV lamp. Evaporation was performed in vacuo (rotating evaporator). Sodium sulfate was always used as the drying agent.

**2-Bromo-3-chloroaniline (12).** A solution of 2-bromo-3-chloronitrobenzene (**11**)<sup>20</sup> (3.94 g, 16.7 mmol) in methanol (170 mL) was treated with 0.013 g (0.048 mmol) of FeCl<sub>3</sub>·6H<sub>2</sub>O and 0.884 g of activated charcoal. The mixture was heated to 80 °C; hydrazine monohydrate was then added dropwise (13 mL, 260 mmol), and the resulting suspension was stirred at the same temperature overnight. The reaction mixture was then cooled to RT, filtered, and concentrated under vacuum. The crude residue was dissolved in chloroform, washed with brine, dried, and concentrated to give **12** as a yellow solid (2.96, 86% yield); <sup>1</sup>H NMR (CDCl<sub>3</sub>)  $\delta$  (ppm): 4.26 (bs, 2H), 6.65 (dd, 1H,  $J = 8.1, 1.5$  Hz), 6.84 (dd, 1H,  $J = 8.1, 1.5$  Hz), 7.02 (t, 1H,  $J = 8.0$  Hz). MS  $m/z$  205 (M<sup>+</sup>).

**2-Bromo-3-chloro-*N*-trifluoroacetylaniline (13).** A solution of **12** (2.96 g, 14.4 mmol) in acetone (35 mL) was treated under nitrogen with potassium carbonate (2.97 g, 21.5 mmol) and 4.0 mL of trifluoroacetic anhydride (28 mmol), and it was stirred at RT overnight. An additional amount of trifluoroacetic anhydride (2 mL, 14 mmol) was added, and stirring was continued for 6 h, and then the mixture was diluted with water and extracted with Et<sub>2</sub>O. The organic phase was dried and concentrated to give **13** (4.33 g, 99% yield) as a yellow solid that was used in the next step without further purification; <sup>1</sup>H NMR (CDCl<sub>3</sub>)  $\delta$  (ppm): 7.34–7.39 (m, 2H), 8.21–8.30 (m, 1H), 8.57 (bs, 1H). MS  $m/z$  301 (M<sup>+</sup>).

**2-Bromo-3-chloro-*N*-methyl-*N*-trifluoroacetylaniline (14).** A solution of **13** (4.33 g, 14.3 mmol) in DMF (36 mL) was treated under nitrogen with potassium carbonate (3.97 g, 28.7 mmol) and 1.8 mL of iodomethane (28 mmol), and it was stirred at RT for 3 h. Two additional amounts of iodomethane (each 0.5 mL, 8 mmol) were added, and stirring was continued for 3 h, and then the mixture was diluted with water and extracted with ethyl acetate. The organic

phase was dried and concentrated to give **14** (4.07 g, 90% yield) as an orange solid that was used in the next step without further purification;  $^1\text{H NMR}$  ( $\text{CDCl}_3$ )  $\delta$  (ppm): 3.31 (s, 3H), 7.21–7.40 (m, 2H), 7.54 (dd, 1H,  $J = 7.9, 1.6$  Hz). MS  $m/z$  315 ( $\text{M}^+$ ).

**2-Bromo-3-chloro-N-methylaniline (15)**. A solution of **14** (4.07 g, 12.9 mmol) in methanol (135 mL) and water (55 mL) was treated with potassium carbonate (11.2 g, 81.2 mmol), and it was stirred at RT overnight. The reaction mixture was then diluted with water and extracted with  $\text{Et}_2\text{O}$ . The organic phase was dried and concentrated to give **15** (2.81 g, 99% yield) as a yellowish solid that was used in the next step without further purification;  $^1\text{H NMR}$  ( $\text{CDCl}_3$ )  $\delta$  (ppm): 2.90 (d, 1H,  $J = 5.1$  Hz), 4.57 (bs, 1H), 6.49 (dd, 1H,  $J = 8.2, 1.3$  Hz), 6.80 (dd, 1H,  $J = 8.0, 1.4$  Hz), 7.13 (t, 1H,  $J = 8.1$  Hz). MS  $m/z$  219 ( $\text{M}^+$ ).

**N-Allyl-2-bromo-3-chloro-N-methylaniline (16)**. A solution of **15** (2.81 g, 12.8 mmol) in acetonitrile (13 mL) was treated with potassium carbonate (3.2 g, 23 mmol), and it was heated at 50 °C. A solution of allyl bromide (6.5 mL, 77 mmol) in acetonitrile (16 mL) was then added dropwise through a dropping funnel, and after the addition was completed, the reaction mixture was heated to 100 °C for 4 h. TLC analysis still showed the presence of starting material; therefore, more allyl bromide (6.5 mL) in acetonitrile (16 mL) was added, and the mixture was kept under stirring at 100 °C overnight. The reaction mixture was then cooled to RT, and the resulting suspension was filtered under vacuum. The residue was extracted with  $\text{Et}_2\text{O}$ , and the combined filtrates were concentrated under vacuum to give **16** (3.33 g, 99% yield) as a yellow oil that was used in the next step without further purification;  $^1\text{H NMR}$  ( $\text{CDCl}_3$ )  $\delta$  (ppm): 2.73 (s, 3H), 3.60 (d, 2H,  $J = 6.0$  Hz), 5.16–5.23 (m, 1H), 5.29 (dq, 1H,  $J = 17.0, 1.6$  Hz), 5.92 (ddt, 1H,  $J = 17.2, 10.2, 6.0$  Hz), 6.94–7.01 (m, 1H), 7.12–7.19 (m, 2H). MS  $m/z$  259 ( $\text{M}^+$ ).

**6-Allyl-2-bromo-3-chloro-N-methylaniline (17)**. A solution of **16** (3.33 g, 12.8 mmol) in sulfolane (4 mL) was treated under nitrogen with  $\text{BF}_3 \cdot \text{Et}_2\text{O}$  (5.7 mL, 45 mmol), and it was heated at 120 °C under stirring overnight. After cooling to RT, the mixture was diluted with water, neutralized with a 1 N aqueous NaOH solution, and extracted with  $\text{Et}_2\text{O}$ . The organic phase was dried and concentrated under vacuum to give a crude product, which was purified by flash chromatography (*n*-hexane/dichloromethane 9:1), yielding pure **17** (2.95 g, 89% yield) as a yellow oil;  $^1\text{H NMR}$  ( $\text{CDCl}_3$ )  $\delta$  (ppm): 2.82 (s, 3H), 3.46 (dt, 2H,  $J = 6.2, 1.6$  Hz), 5.04 (dq, 1H,  $J = 16.8, 1.8$  Hz), 5.14 (dq, 1H,  $J = 10.1, 1.6$  Hz), 5.96 (ddt, 1H,  $J = 16.8, 10.2, 6.4$  Hz), 7.02 (d, 1H,  $J = 8.2$  Hz), 7.07 (d, 1H,  $J = 8.2$  Hz). MS  $m/z$  259 ( $\text{M}^+$ ).

**(E/Z)-2-Bromo-3-chloro-N-methyl-6-(prop-1-enyl)aniline (18)**. A solution of **17** (2.95 g, 11.3 mmol) in DMSO (30 mL) was treated under nitrogen with *t*-BuOK (3.18 g, 28.4 mmol) and stirred at RT for 1 h. The reaction mixture was then quenched with saturated aqueous  $\text{NH}_4\text{Cl}$  and extracted with  $\text{Et}_2\text{O}$ . The organic phase was washed with brine, dried, and concentrated under vacuum, and the crude product was purified by flash chromatography (*n*-hexane/dichloromethane 9:1) to yield pure **18** (1.82 g, 62% yield) as an oil;  $^1\text{H NMR}$  ( $\text{CDCl}_3$ , 9:1 *E/Z* mixture, asterisk denotes minor isomer peaks)  $\delta$  (ppm): 1.78\* (dd, 3H,  $J = 7.0, 1.8$  Hz), 1.91 (dd, 3H,  $J = 6.6, 1.8$  Hz), 2.81 (s, 3H), 2.84\* (s, 3H), 6.11 (dq, 1H,  $J = 15.8, 6.6$  Hz), 6.49–6.58 (m, 1H), 7.00 (d, 1H,  $J = 8.2$  Hz), 7.20 (d, 1H,  $J = 8.4$  Hz). MS  $m/z$  259 ( $\text{M}^+$ ).

**(E/Z)-3-Chloro-N-methyl-2-phenyl-6-(prop-1-enyl)aniline (19a)**. A solution of **18** (453 mg, 1.75 mmol) in toluene (4.5 mL), ethanol (4.5 mL), and 2 M aqueous  $\text{Na}_2\text{CO}_3$  (4.5 mL) was treated under nitrogen with phenylboronic acid (464 mg, 3.81 mmol) and  $\text{Pd}(\text{PPh}_3)_4$  (0.088 mmol), and the mixture was heated to reflux for 20 h. The reaction mixture was then cooled to RT, diluted with water, and extracted with  $\text{Et}_2\text{O}$ . The organic phase was washed with brine, dried, and concentrated under vacuum, and the crude product was purified by flash chromatography (*n*-hexane/dichloromethane 9:1 → 8:2) to yield pure **19a** (180 mg, 40% yield) as a yellow solid: mp 62 °C;  $^1\text{H NMR}$  ( $\text{CDCl}_3$ )  $\delta$  (ppm): 1.90 (dd, 3H,  $J = 6.5, 1.7$  Hz), 2.59 (s, 3H), 6.14 (dq, 1H,  $J = 15.8, 6.4$  Hz), 6.50–6.59 (m,

1H), 7.02 (d, 1H,  $J = 8.4$  Hz), 7.23–7.30 (m, 2H), 7.37–7.53 (m, 4H). MS  $m/z$  257 ( $\text{M}^+$ ).

**(E/Z)-3-Chloro-2-(4-methoxyphenyl)-N-methyl-6-(prop-1-enyl)aniline (19b)**. Compound **18** (910 mg, 3.51 mmol) was submitted to the same procedure described above for the preparation of **19a** by reacting with 4-methoxyphenylboronic acid (0.64 g, 4.2 mmol). Purification of the crude product by flash chromatography (*n*-hexane/dichloromethane 9:1) yielded pure **19b** (0.77 g, 76% yield) as a light yellow solid;  $^1\text{H NMR}$  ( $\text{CDCl}_3$ , 9:1 *E/Z* mixture, asterisk denotes minor isomer peaks)  $\delta$  (ppm): 1.84\* (dd, 3H,  $J = 7.0, 1.8$  Hz), 1.92 (dd, 3H,  $J = 6.6, 1.6$  Hz), 2.60 (s, 3H), 3.87 (s, 3H), 6.13 (dq, 1H,  $J = 15.7, 6.6$  Hz), 6.55 (dq, 1H,  $J = 15.9, 1.6$  Hz), 7.01 (AA'XX', 2H,  $J_{\text{AX}} = 8.8$  Hz,  $J_{\text{AA'XX'}} = 2.3$  Hz), 7.03 (d, 1H,  $J = 8.2$  Hz), 7.18 (AA'XX', 2H,  $J_{\text{AX}} = 8.8$  Hz,  $J_{\text{AA'XX'}} = 2.4$  Hz), 7.26 (d, 1H,  $J = 8.4$  Hz); MS  $m/z$  287 ( $\text{M}^+$ ).

**(E/Z)-3-(4-Methoxyphenyl)-N-methyl-2-phenyl-6-(prop-1-enyl)aniline (20a)**. A solution of **19a** (305 mg, 1.19 mmol) in dioxane (3 mL) was treated with cesium carbonate (658 mg, 2.02 mmol), 4-methoxyphenylboronic acid (270 mg, 1.80 mmol),  $\text{Pd}_2(\text{dba})_3$  (35 mg, 0.038 mmol), and 0.15 mL of a 20% solution of tricyclohexylphosphine (0.10 mmol) in toluene, and the resulting mixture was heated to 80 °C in a sealed vial for 24 h. The reaction mixture was then cooled to RT, diluted with  $\text{Et}_2\text{O}$ , and filtered through a Celite pad. The organic filtrate was concentrated under vacuum, and the crude product was purified by flash chromatography (*n*-hexane/dichloromethane 7:3) to yield pure **20a** (331 mg, 84% yield) as an oil;  $^1\text{H NMR}$  ( $\text{CDCl}_3$ )  $\delta$  (ppm): 1.94 (dd, 3H,  $J = 6.5, 1.6$  Hz), 2.62 (s, 3H), 3.72 (s, 3H), 6.20 (dq, 1H,  $J = 15.8, 6.6$  Hz), 6.64 (AA'XX', 2H,  $J_{\text{AX}} = 8.6$  Hz,  $J_{\text{AA'XX'}} = 2.4$  Hz), 6.67–6.71 (m, 1H), 6.94 (AA'XX', 2H,  $J_{\text{AX}} = 8.8$  Hz,  $J_{\text{AA'XX'}} = 2.4$  Hz), 6.97–7.00 (m, 1H), 7.06–7.28 (m, 5H), 7.42 (d, 1H,  $J = 7.6$  Hz). MS  $m/z$  329 ( $\text{M}^+$ ).

**(E/Z)-2-(4-Methoxyphenyl)-N-methyl-3-phenyl-6-(prop-1-enyl)aniline (20b)**. Compound **19b** (0.77 g, 2.7 mmol) was submitted to the same procedure described above for the preparation of **20a**, by reacting with phenylboronic acid (0.77 g, 4.0 mmol). Purification of the crude product by flash chromatography (*n*-hexane/dichloromethane 1:1) yielded pure **20b** (0.82 g, 93% yield) as a yellow solid;  $^1\text{H NMR}$  ( $\text{CDCl}_3$ )  $\delta$  (ppm): 1.95 (dd, 3H,  $J = 6.6, 1.6$  Hz), 2.64 (s, 3H), 3.78 (s, 3H), 6.21 (dq, 1H,  $J = 15.7, 6.4$  Hz), 6.64–6.73 (m, 1H), 6.80 (AA'XX', 2H,  $J_{\text{AX}} = 8.6$  Hz,  $J_{\text{AA'XX'}} = 2.4$  Hz), 6.98–7.14 (m, 8H), 7.42 (d, 1H,  $J = 7.9$  Hz). MS  $m/z$  329 ( $\text{M}^+$ ).

**4-(4-Methoxyphenyl)-N-methyl-3-phenylanthranaldehyde (21a)**. A solution of **20a** (315 mg, 0.958 mmol) in dioxane (7 mL) was treated dropwise with water (4 mL), then with sodium periodate (1.0 g) and 0.05 mL of a 2.5% solution of osmium tetroxide in *tert*-butyl alcohol (0.05 mmol). The mixture was stirred at RT for 7 h, and then most of the solvent was removed under vacuum, and the residue was diluted with water and repeatedly extracted with chloroform. The combined organic phase was washed with aqueous  $\text{Na}_2\text{S}_2\text{O}_3$  and brine and then dried and concentrated under vacuum. The resulting crude residue was purified by flash chromatography (*n*-hexane/ethyl acetate 9:1) to yield pure **21a** (88 mg, 29% yield) as a yellow solid: mp = 120 °C;  $^1\text{H NMR}$  ( $\text{CDCl}_3$ )  $\delta$  (ppm): 2.26 (s, 3H), 3.74 (s, 3H), 6.66 (AA'XX', 2H,  $J_{\text{AX}} = 8.8$  Hz,  $J_{\text{AA'XX'}} = 2.5$  Hz), 6.76 (d, 1H,  $J = 8.0$  Hz), 6.88 (AA'XX', 2H,  $J_{\text{AX}} = 8.8$  Hz,  $J_{\text{AA'XX'}} = 2.5$  Hz), 7.06–7.22 (m, 5H), 7.49 (d, 1H,  $J = 7.9$  Hz), 8.25 (bs, 1H), 9.88 (s, 1H). MS  $m/z$  317 ( $\text{M}^+$ ).

**3-(4-Methoxyphenyl)-N-methyl-4-phenylanthranaldehyde (21b)**. Compound **20b** (0.21 g, 0.64 mmol) was submitted to the same procedure described above for the preparation of **21a**. Purification of the crude product by flash chromatography (*n*-hexane/ethyl acetate 9:1) yielded pure **21b** (75 mg, 37% yield) as a yellow solid;  $^1\text{H NMR}$  ( $\text{CDCl}_3$ )  $\delta$  (ppm): 2.31 (s, 3H), 3.76 (s, 3H), 6.71 (AA'XX', 2H,  $J_{\text{AX}} = 8.8$  Hz,  $J_{\text{AA'XX'}} = 2.5$  Hz), 6.77 (d, 1H,  $J = 7.9$  Hz), 6.95–7.02 (m, 4H), 7.11–7.16 (m, 3H), 7.49 (d, 1H,  $J = 8.1$  Hz), 9.89 (s, 1H). MS  $m/z$  317 ( $\text{M}^+$ ).

**4-(4-Hydroxyphenyl)-N-methyl-3-phenylanthranaldehyde (22a)**. A solution of **21a** (137 mg, 0.430 mmol) in dichloromethane (9 mL) was cooled under nitrogen to –78 °C and treated dropwise



with a 1 M solution of  $\text{BBR}_3$  in dichloromethane (1.1 mL, 1.1 mmol), and the resulting solution was stirred at the same temperature for 5 min and at RT for 3 h. The mixture was then diluted with water and extracted with ethyl acetate. The organic phase was dried and concentrated. The crude product was purified by flash chromatography (*n*-hexane/ethyl acetate 7:3) to yield pure **22a** (79 mg, 61% yield) as a yellow solid: mp 105 °C;  $^1\text{H NMR}$  ( $\text{CDCl}_3$ )  $\delta$  (ppm): 2.27 (s, 3H), 6.59 (AA'XX', 2H,  $J_{\text{AX}} = 8.8$  Hz,  $J_{\text{AA'XX'}} = 2.1$  Hz), 6.77 (d, 1H,  $J = 8.0$  Hz), 6.84 (AA'XX', 2H,  $J_{\text{AX}} = 8.8$  Hz,  $J_{\text{AA'XX'}} = 2.1$  Hz), 7.07–7.20 (m, 5H), 7.49 (d, 1H,  $J = 7.9$  Hz), 9.88 (s, 1H). MS  $m/z$  303 ( $\text{M}^+$ ).

**3-(4-Hydroxyphenyl)-*N*-methyl-4-phenylanthranaldehyde (22b)**. Compound **21b** (0.060 g, 0.19 mmol) was submitted to the same procedure described above for the preparation of **22a**. Purification of the crude product by flash chromatography (*n*-hexane/ethyl acetate 8:2) yielded pure **22b** (31 mg, 53% yield) as a yellow solid;  $^1\text{H NMR}$  ( $\text{CDCl}_3$ )  $\delta$  (ppm): 2.33 (s, 3H), 4.80 (bs, 1H), 6.65 (AA'XX', 2H,  $J_{\text{AX}} = 8.8$  Hz,  $J_{\text{AA'XX'}} = 2.4$  Hz), 6.78 (d, 1H,  $J = 7.9$  Hz), 6.92–7.00 (m, 4H), 7.11–7.16 (m, 3H), 7.50 (d, 1H,  $J = 8.1$  Hz), 9.89 (s, 1H). MS  $m/z$  303 ( $\text{M}^+$ ).

**4-(4-Hydroxyphenyl)-*N*-methyl-3-phenylanthranaldehyde (3)**. A solution of **22a** (25 mg, 0.082 mmol) in methanol (2 mL) was treated with hydroxylamine hydrochloride (12 mg, 0.17 mmol), and the mixture was heated to 50 °C for 1 h. After being cooled to RT, the solvent was removed under vacuum, and the crude product was purified by column chromatography (*n*-hexane/ethyl acetate 7:3) to yield pure **3** (18 mg, 70% yield) as an off-white solid: mp 42 °C;  $^1\text{H NMR}$  ( $\text{CDCl}_3$ )  $\delta$  (ppm): 2.39 (s, 3H), 6.58 (AA'XX', 2H,  $J_{\text{AX}} = 8.8$  Hz,  $J_{\text{AA'XX'}} = 2.5$  Hz), 6.85 (AA'XX', 2H,  $J_{\text{AX}} = 8.8$  Hz,  $J_{\text{AA'XX'}} = 2.5$  Hz), 6.90 (d, 1H,  $J = 8.0$  Hz), 7.09–7.24 (m, 5H), 7.37 (d, 1H,  $J = 7.9$  Hz), 8.36 (s, 1H). MS  $m/z$  318 ( $\text{M}^+$ ). Anal. ( $\text{C}_{20}\text{H}_{18}\text{N}_2\text{O}_2$ ) C, H, N.

**3-(4-Hydroxyphenyl)-*N*-methyl-4-phenylanthranaldehyde (4)**. Compound **22b** (21 mg, 0.068 mmol) was submitted to the same procedure described above for the preparation of **3**. Purification of the crude product by column chromatography (*n*-hexane/ethyl acetate 7:3) yielded pure **4** (18 mg, 82% yield) as a white solid: mp 172 °C;  $^1\text{H NMR}$  ( $\text{CDCl}_3$ )  $\delta$  (ppm): 2.42 (s, 3H), 6.68 (AA'XX', 2H,  $J_{\text{AX}} = 8.6$  Hz,  $J_{\text{AA'XX'}} = 2.3$  Hz), 6.89 (d, 1H,  $J = 7.9$  Hz), 6.97 (AA'XX', 2H,  $J_{\text{AX}} = 8.6$  Hz,  $J_{\text{AA'XX'}} = 2.3$  Hz), 7.00–7.02 (m, 2H), 7.12–7.15 (m, 3H), 7.36 (d, 1H,  $J = 7.9$  Hz), 8.36 (s, 1H). MS  $m/z$ : 318 ( $\text{M}^+$ , 20), 301 ( $\text{M}^+ - \text{OH}$ , 100), 300 ( $\text{M}^+ - \text{H}_2\text{O}$ , 29), 286 ( $\text{M}^+ - \text{NHOH}$ , 21). Anal. ( $\text{C}_{20}\text{H}_{18}\text{N}_2\text{O}_2$ ) C, H, N.

**Synthesis of (E/Z)-2,3-Diaryl-*N*-methyl-6-(prop-1-enyl)-anilines (24a–d). General Procedure.** A solution of **23**<sup>16</sup> (2 mmol) in dioxane (3 mL) was treated under nitrogen with cesium carbonate (4 mmol), the appropriate arylboronic acid (2.8 mmol),  $\text{Pd}_2(\text{dba})_3$  (0.060 mmol), and a 20% solution of tricyclohexylphosphine (0.14 mmol) in toluene. The resulting mixture was heated to 80 °C in a sealed vial for 16 h. The reaction mixture was then cooled to RT, diluted with  $\text{Et}_2\text{O}$ , and filtered through a Celite pad. The solvent was removed under vacuum, and the resulting crude mixture was submitted again to the same treatment described above. The crude product derived from the second step was purified by column chromatography, eluting with the indicated eluent to obtain compounds **24a–d** as *E/Z* mixtures.

**(E/Z)-2,3-Bis(4-methoxyphenyl)-*N*-methyl-6-(prop-1-enyl)-aniline (24a)**. Eluent: *n*-hexane/dichloromethane 1:1; yield 67%; off-white solid: mp 126–130 °C;  $^1\text{H NMR}$  ( $\text{CDCl}_3$ , 9:1 *E/Z* mixture, asterisk denotes minor isomer peaks)  $\delta$  (ppm): 1.95 (dd, 3H,  $J = 6.6, 1.6$  Hz), 2.62\* (s, 3H), 2.64 (s, 3H), 3.74 (s, 3H), 3.76\* (s, 3H), 3.79 (s, 3H), 3.85\* (s, 3H), 6.20 (dq, 1H,  $J = 15.5, 6.6$  Hz), 6.67 (AA'XX', 2H,  $J_{\text{AX}} = 8.8$  Hz,  $J_{\text{AA'XX'}} = 2.4$  Hz), 6.73–6.78 (m, 1H), 6.82 (AA'XX', 2H,  $J_{\text{AX}} = 8.6$  Hz,  $J_{\text{AA'XX'}} = 2.4$  Hz), 6.95 (AA'XX', 2H,  $J_{\text{AX}} = 8.6$  Hz,  $J_{\text{AA'XX'}} = 2.4$  Hz), 7.01 (AA'XX', 2H,  $J_{\text{AX}} = 8.7$  Hz,  $J_{\text{AA'XX'}} = 2.4$  Hz), 7.41 (d, 1H,  $J = 7.9$  Hz). MS  $m/z$  359 ( $\text{M}^+$ ).

**(E/Z)-2,3-Bis(3-methoxyphenyl)-*N*-methyl-6-(prop-1-enyl)-aniline (24b)**. Eluent: *n*-hexane/dichloromethane 1:1; yield 38%; yellow oil;  $^1\text{H NMR}$  ( $\text{CDCl}_3$ )  $\delta$  (ppm): 1.95 (dd, 3H,  $J = 6.6, 1.6$

Hz), 2.66 (s, 3H), 3.58 (s, 3H), 3.66 (s, 3H), 6.20 (dq, 1H,  $J = 15.6, 6.6$  Hz), 6.60–6.86 (m, 6H), 7.0–7.24 (m, 4H), 7.44 (d, 1H,  $J = 8.1$  Hz). MS  $m/z$  359 ( $\text{M}^+$ ).

**(E/Z)-2,3-Bis(4-methylphenyl)-*N*-methyl-6-(prop-1-enyl)-aniline (24c)**. Eluent: *n*-hexane/dichloromethane 7:3; yield 62%; off-white solid: mp 39–41 °C;  $^1\text{H NMR}$  ( $\text{CDCl}_3$ )  $\delta$  (ppm): 2.02 (dd, 3H,  $J = 6.6, 1.6$  Hz), 2.26 (s, 3H), 2.29 (s, 3H), 2.35 (s, 3H), 6.28–6.39 (m, 1H), 6.70–6.73 (m, 1H), 6.87–7.05 (m, 8H), 7.70 (d, 1H,  $J = 8.1$  Hz), 7.59 (d, 1H,  $J = 8.1$  Hz). MS  $m/z$  327 ( $\text{M}^+$ ).

**(E/Z)-2,3-Bis(3-methylphenyl)-*N*-methyl-6-(prop-1-enyl)-aniline (24d)**. Eluent: *n*-hexane/dichloromethane 7:3; yield 35%; yellow oil;  $^1\text{H NMR}$  ( $\text{CDCl}_3$ )  $\delta$  (ppm): 1.92 (dd, 3H,  $J = 6.5, 1.6$  Hz), 2.18 (s, 3H), 2.41 (s, 3H), 2.94 (s, 3H), 6.08 (dq, 1H,  $J = 15.4, 6.4$  Hz), 6.42 (dq, 1H,  $J = 15.4, 1.6$  Hz), 6.80–7.41 (m, 10H). MS  $m/z$  327 ( $\text{M}^+$ ).

**Synthesis of 2,3-Diaryl-*N*-methylanthranaldehydes (25a–d). General Procedure.** A solution of the appropriate olefin precursor (**24a–d**) (1.25 mmol) in dioxane (15 mL) was treated dropwise with water (7 mL), then with sodium periodate (1.2 g), and 0.13 mL of a 2.5% solution of osmium tetroxide in *tert*-butyl alcohol. The mixture was stirred at RT for 5 h, then most of the solvent was removed under vacuum, and the residue was diluted with water and repeatedly extracted with chloroform. The combined organic phase was washed with aqueous  $\text{Na}_2\text{S}_2\text{O}_3$  and brine, and then dried and concentrated under vacuum. The resulting crude residue was purified by flash chromatography, eluting with the indicated eluent to obtain compounds **25a–d**.

**2,3-Bis(4-methoxyphenyl)-*N*-methylanthranaldehyde (25a)**. Eluent: *n*-hexane/EtOAc 8:2; yield 34%; off-white solid: mp 105 °C;  $^1\text{H NMR}$  ( $\text{CDCl}_3$ )  $\delta$  (ppm): 2.33 (s, 3H), 3.75 (s, 3H), 3.78 (s, 3H), 6.69 (AA'XX', 2H,  $J_{\text{AX}} = 9.0$  Hz,  $J_{\text{AA'XX'}} = 2.3$  Hz), 6.75 (AA'XX', 2H,  $J_{\text{AX}} = 8.8$  Hz,  $J_{\text{AA'XX'}} = 2.4$  Hz), 6.85 (d, 1H,  $J = 7.9$  Hz), 6.91 (AA'XX', 2H,  $J_{\text{AX}} = 9.0$  Hz,  $J_{\text{AA'XX'}} = 2.4$  Hz), 7.03 (AA'XX', 2H,  $J_{\text{AX}} = 8.6$  Hz,  $J_{\text{AA'XX'}} = 2.5$  Hz), 7.51 (d, 1H,  $J = 7.9$  Hz), 9.89 (s, 1H). MS  $m/z$  347 ( $\text{M}^+$ ).

**2,3-Bis(3-methoxyphenyl)-*N*-methylanthranaldehyde (25b)**. Eluent: *n*-hexane/EtOAc 8:2; yield 32%; oil;  $^1\text{H NMR}$  ( $\text{CDCl}_3$ )  $\delta$  (ppm): 2.49 (s, 3H), 3.59 (s, 3H), 3.72 (s, 3H), 6.61–8.04 (m, 10H), 9.98 (s, 1H). MS  $m/z$  347 ( $\text{M}^+$ ).

**2,3-Bis(4-tolyl)-*N*-methylanthranaldehyde (25c)**. Eluent: *n*-hexane/ $\text{Et}_2\text{O}$  8:2; yield 38%; yellow solid: mp 110–112 °C;  $^1\text{H NMR}$  ( $\text{CDCl}_3$ )  $\delta$  (ppm): 2.28 (s, 3H), 2.32 (s, 3H), 2.50 (s, 3H), 6.87–7.34 (m, 9H), 7.63 (d, 1H,  $J = 7.9$  Hz), 7.98 (d, 1H,  $J = 8.0$  Hz), 9.90 (s, 1H). MS  $m/z$  315 ( $\text{M}^+$ ).

**2,3-Bis(3-tolyl)-*N*-methylanthranaldehyde (25d)**. Eluent: *n*-hexane/EtOAc 9:1; yield 42%; oil;  $^1\text{H NMR}$  ( $\text{CDCl}_3$ )  $\delta$  (ppm): 2.19 (s, 3H), 2.22 (s, 3H), 2.30 (s, 3H), 6.72–6.87 (m, 3H), 6.76 (d, 1H,  $J = 8.0$  Hz), 6.94–7.03 (m, 5H), 7.48 (d, 1H,  $J = 7.9$  Hz), 9.87 (s, 1H). MS  $m/z$  315 ( $\text{M}^+$ ).

**Synthesis of Hydroxylated 2,3-Diaryl-*N*-methylanthranaldehydes (25e,f). General Procedure.** A solution of the appropriate methyl-ether precursor (**25a,b**) (0.27 mmol) in anhydrous dichloromethane (9 mL) was cooled under nitrogen to –78 °C and treated dropwise with a 1 M solution of  $\text{BBR}_3$  in dichloromethane (1.2 mL, 1.2 mmol), and the resulting solution was stirred at the same temperature for 5 min and at RT for 2 h. The mixture was then diluted with water and extracted with ethyl acetate. The organic phase was dried and concentrated. The resulting crude residue was purified by flash chromatography, eluting with the indicated eluent to obtain compounds **25e** and **f**.

**2,3-Bis(4-hydroxyphenyl)-*N*-methylanthranaldehyde (25e)**. Eluent: *n*-hexane/EtOAc 1:1; yield 53%; white solid: mp 95 °C;  $^1\text{H NMR}$  (acetone- $d_6$ )  $\delta$  (ppm): 2.33 (d, 3H,  $J = 5.3$  Hz), 6.63 (AA'XX', 2H,  $J_{\text{AX}} = 8.6$  Hz,  $J_{\text{AA'XX'}} = 2.4$  Hz), 6.69–6.77 (m, 3H), 6.86 (AA'XX', 2H,  $J_{\text{AX}} = 8.6$  Hz,  $J_{\text{AA'XX'}} = 2.5$  Hz), 6.93 (AA'XX', 2H,  $J_{\text{AX}} = 8.6$  Hz,  $J_{\text{AA'XX'}} = 2.5$  Hz), 7.58 (d, 1H,  $J = 8.1$  Hz), 8.27 (s, 1H), 8.32 (s, 1H), 9.91 (s, 1H). MS  $m/z$  319 ( $\text{M}^+$ ).

**2,3-Bis(3-hydroxyphenyl)-*N*-methylanthranaldehyde (25f)**. Eluent: *n*-hexane/EtOAc 7:3; yield 41%; light yellow solid: mp 95 °C;  $^1\text{H NMR}$  (acetone- $d_6$ )  $\delta$  (ppm): 2.35 (d, 3H,  $J = 4.8$  Hz), 6.46–6.70 (m, 4H), 6.72 (d, 1H,  $J = 7.9$  Hz), 6.92–7.07 (m, 4H),

7.60 (d, 1H,  $J = 8.0$  Hz), 8.34 (s, 1H), 8.36 (s, 1H), 9.92 (s, 1H). MS  $m/z$  319 ( $M^+$ ).

**Synthesis of 2,3-Diaryl-*N*-methylanthranlyldoximes (5–10).**  
**General Procedure.** A solution of the appropriate aldehyde precursor (**25a–f**) (0.17 mmol) in methanol (5 mL) was treated with hydroxylamine hydrochloride (24 mg, 0.35 mmol), and the mixture was heated to 50 °C for 1 h. After being cooled to RT, the solvent was removed under vacuum, and the resulting crude residue was purified by flash chromatography, eluting with the indicated eluent to obtain compounds **5–10**.

**2,3-Bis(4-hydroxyphenyl)-*N*-methylanthranlyldoxime (5).** Eluent: *n*-hexane/EtOAc 1:1; yield 38%; white solid: mp 98–100 °C;  $^1\text{H}$  NMR (acetone- $d_6$ )  $\delta$  (ppm): 2.34 (s, 3H), 6.61 (AA'XX', 2H,  $J_{AX} = 8.6$  Hz,  $J_{AA'/XX'} = 2.5$  Hz), 6.72 (AA'XX', 2H,  $J_{AX} = 8.7$  Hz,  $J_{AA'/XX'} = 2.5$  Hz), 6.80 (d, 1H,  $J = 8.1$  Hz), 6.84 (AA'XX', 2H,  $J_{AX} = 8.6$  Hz,  $J_{AA'/XX'} = 2.4$  Hz), 6.93 (AA'XX', 2H,  $J_{AX} = 8.6$  Hz,  $J_{AA'/XX'} = 2.4$  Hz), 7.37 (d, 1H,  $J = 8.1$  Hz), 8.19 (bs, 1H), 8.28 (bs, 1H), 8.34 (s, 1H), 10.21 (bs, 1H). MS  $m/z$  334 ( $M^+$ ). Anal. ( $\text{C}_{20}\text{H}_{18}\text{N}_2\text{O}_3$ ) C, H, N.

**2,3-Bis(3-hydroxyphenyl)-*N*-methylanthranlyldoxime (6).** Eluent: *n*-hexane/EtOAc 1:1; yield 43%; glass;  $^1\text{H}$  NMR (acetone- $d_6$ )  $\delta$  (ppm): 2.36 (s, 3H), 6.46–6.69 (m, 4H), 6.78 (d, 1H,  $J = 7.9$  Hz), 6.90–7.09 (m, 4H), 7.39 (d, 1H,  $J = 8.0$  Hz), 8.17 (s, 1H), 8.23 (s, 1H), 8.35 (s, 1H), 10.27 (s, 1H). MS  $m/z$  334 ( $M^+$ ). Anal. ( $\text{C}_{20}\text{H}_{18}\text{N}_2\text{O}_3$ ) C, H, N.

**2,3-Bis(4-methoxyphenyl)-*N*-methylanthranlyldoxime (7).** Eluent: *n*-hexane/EtOAc 7:3; yield 70%; off-white solid: mp 175–177 °C;  $^1\text{H}$  NMR ( $\text{CDCl}_3$ )  $\delta$  (ppm): 2.48 (s, 3H), 3.75 (s, 3H), 3.80 (s, 3H), 6.69 (AA'XX', 2H,  $J_{AX} = 8.8$  Hz,  $J_{AA'/XX'} = 2.4$  Hz), 6.82 (AA'XX', 2H,  $J_{AX} = 8.6$  Hz,  $J_{AA'/XX'} = 2.2$  Hz), 6.92 (AA'XX', 2H,  $J_{AX} = 8.8$  Hz,  $J_{AA'/XX'} = 2.4$  Hz), 7.06 (d, 1H,  $J = 7.9$  Hz), 7.08 (AA'XX', 2H,  $J_{AX} = 8.6$  Hz,  $J_{AA'/XX'} = 2.1$  Hz), 7.37 (d, 1H,  $J = 8.0$  Hz), 8.33 (s, 1H). MS  $m/z$  362 ( $M^+$ ). Anal. ( $\text{C}_{22}\text{H}_{22}\text{N}_2\text{O}_3$ ) C, H, N.

**2,3-Bis(3-methoxyphenyl)-*N*-methylanthranlyldoxime (8).** Eluent: *n*-hexane/EtOAc 7:3; yield 41%; light yellow solid: mp 45–48 °C;  $^1\text{H}$  NMR ( $\text{CDCl}_3$ )  $\delta$  (ppm): 2.48 (s, 3H), 3.58 (s, 3H), 3.66 (s, 3H), 6.52–6.78 (m, 4H), 6.98 (d, 1H,  $J = 7.9$  Hz), 7.03–7.20 (m, 4H), 7.39 (d, 1H,  $J = 7.9$  Hz), 8.36 (s, 1H). MS  $m/z$  362 ( $M^+$ ). Anal. ( $\text{C}_{22}\text{H}_{22}\text{N}_2\text{O}_3$ ) C, H, N.

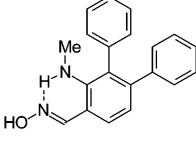
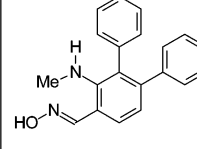
**2,3-Bis(4-tolyl)-*N*-methylanthranlyldoxime (9).** Eluent: *n*-hexane/EtOAc 8:2; yield 52%; light yellow glass;  $^1\text{H}$  NMR ( $\text{CDCl}_3$ )  $\delta$  (ppm): 2.26 (s, 3H), 2.31 (s, 3H), 2.43 (s, 3H), 6.87–7.10 (m, 9H), 7.40 (d, 1H,  $J = 8.1$  Hz), 8.36 (s, 1H). MS  $m/z$  330 ( $M^+$ ). Anal. ( $\text{C}_{22}\text{H}_{22}\text{N}_2\text{O}$ ) C, H, N.

**2,3-Bis(3-tolyl)-*N*-methylanthranlyldoxime (10).** Eluent: *n*-hexane/EtOAc 9:1; yield 68%; light yellow glass;  $^1\text{H}$  NMR ( $\text{CDCl}_3$ )  $\delta$  (ppm): 2.19 (s, 3H), 2.24 (s, 3H), 2.44 (s, 3H), 6.74–6.78 (m, 1H), 6.84–6.99 (m, 7H), 7.03–7.13 (m, 1H), 7.39 (d, 1H,  $J = 8.0$  Hz), 8.37 (s, 1H). MS  $m/z$  330 ( $M^+$ ). Anal. ( $\text{C}_{22}\text{H}_{22}\text{N}_2\text{O}$ ) C, H, N.

**Biological Methods.** Purified human full-length ER $\alpha$  and ER $\beta$  were obtained from PanVera (Madison, WI). Cell culture media were purchased from Gibco BRL (Grand Island, NY). Calf serum was obtained from Hyclone Laboratories, Inc. (Logan, UT), and fetal calf serum was purchased from Atlanta Biologicals (Atlanta, GA). The luciferase assay system was from Promega (Madison, WI). The expression vectors for human ER $\alpha$  (pCMV5-hER $\alpha$ ) and human ER $\beta$  (pCMV5-ER $\beta$ ) were constructed previously as described.<sup>34,35</sup> The estrogen responsive reporter plasmid was (ERE)<sub>2</sub>-pS2-Luc, was constructed by inserting the (ERE)<sub>2</sub>-pS2 fragment from (ERE)<sub>2</sub>-pS2-CAT into the *Mlu*I/*Bgl*II sites of the pGL3-Basic vector (Promega, Madison, WI). The plasmid pCMV $\beta$  (Clontech, Palo Alto, CA), which contains the  $\beta$ -galactosidase gene, was used as an internal control for transfection efficiency.

**Estrogen Receptor Binding Assays.** Relative binding affinities were determined by competitive radiometric binding assays using 10 nM [ $^3\text{H}$ ]E<sub>2</sub> as a tracer, using previously described methods.<sup>22,23</sup> The source of ERs was purified full-length human ER $\alpha$  and ER $\beta$  purchased from Pan Vera (Madison, WI). Incubations were done at 0 °C for 18–24 h, and hydroxylapatite was used to absorb the purified receptor–ligand complexes (human ERs).<sup>23</sup> The binding

**Table 5.** Energy Difference between the Two Optimized Conformations of Compound **2b**

	
Energy ( $E_{\text{conf. a}} - E_{\text{conf. b}}$ ) = -4.18 Kcal/mol	

affinities are expressed as relative binding affinity (RBA) values, where the RBA of estradiol is 100%; under these conditions, the  $K_d$  of estradiol for ER $\alpha$  is ca. 0.2 nM, and for ER $\beta$  0.5 nM. The determination of these RBA values is reproducible in separate experiments with a CV of 0.3, and the values shown represent the average  $\pm$  range or SD of two, three, or more separate determinations, respectively.

**Computational Details.** Published coordinates for ER $\alpha$  (1G50<sup>24</sup>) and ER $\beta$  (1X7J<sup>25</sup>) were obtained from the Protein Data Bank.<sup>36</sup> In ER $\beta$ , the missed loop M410-N421 was constructed through the loop optimization method of the Modeller program, using 1QKN<sup>5</sup> as the template.

For ER $\alpha$  and ER $\beta$ , the 1G50 and 1X7J reference numbering, was used, respectively; when the amino acid was referred to both receptors, the ER $\beta$  numbering was indicated in parentheses.

**Analysis of the Compound's Geometry.** A conformational search revealed the presence of two low energetic conformations (Table 5), and conformation **a** showed an intramolecular H bond and the formation of a pseudocycle.

To measure the different stabilities of the two conformations and the strength of the intramolecular H bond, both conformations were optimized using the B3LYP/6-31G+\* method. The energy difference between the two optimized systems was about 4 kcal/mol, and this value gave us an idea of the strength of the intramolecular H bond and the better energetic stability of conformation **a**.

**Automated Docking Procedure.** The ligands were submitted to a conformational search of 1000 steps with an energy window for saving the structure of 2 kcal/mol by means of the MACRO-MODEL program.<sup>37</sup> The algorithm used was the Monte Carlo method with MMFFs as the force field and a distance-dependent dielectric constant of 1.0. The first conformation that showed the intramolecular H bond was then minimized using the conjugated gradient method until a convergence value of 0.05 kcal/Å<sup>3</sup>·mol, using the same force field and dielectric constant used for the conformational search.

Automated docking was carried out by means of the program AUTODOCK 3.0;<sup>28</sup> AUTODOCK TOOLS<sup>38</sup> was used to identify the torsion angles in the ligands, add the solvent model, and assign the Kollman and the Gasteiger partial atomic charges to the protein and the ligands, respectively. The regions of interest used by AUTODOCK were defined by considering estradiol into both receptors as the central group; in particular, a grid of 46, 44, and 44 points in the  $x$ ,  $y$ , and  $z$  directions was constructed centered on the center of mass of this compound. A grid spacing of 0.375 Å and a distance-dependent function of the dielectric constant were used for the energetic map calculations.

Using the Lamarckian Genetic Algorithm, the docked compounds were subjected to 100 runs of the AUTODOCK search in which the default values of the other parameters were used. Cluster analysis was performed on the results using an RMS tolerance of 1.0 Å.

**MD Simulations.** All simulations were performed using AMBER 8.0.<sup>39</sup> MD simulations were carried out using the parm94 force field at 300 K. An explicit solvent model TIP3P water was used, and the complexes were solvated with a 10 Å water cap. Sodium ions were added as counterions to neutralize the system. Prior to MD simulations, two steps of minimization were carried out; in the first stage, we kept the protein fixed with a constraint of 500 kcal/mol, and we minimized the positions of the water molecules; then in

the second stage, we minimized the entire system, applying a constraint of 20 kcal/mol on the  $\alpha$  carbon. The two minimization stages consisted of 5000 steps in which the first 1000 were steepest descent (SD) and the last 4000 conjugate gradient (CG). Molecular dynamics trajectories were run using the minimized structure as a starting input. The time step of the simulations was 2.0 fs with a cutoff of 12 Å for the nonbonded interaction, and SHAKE was employed to keep all bonds involving hydrogen atoms rigid. Constant volume was carried out for 100 ps, during which the temperature was raised from 0 to 300 K (using the Langevin dynamics method); then 500 ps (800 ps for the ER $\alpha$  and ER $\beta$  complexed with estradiol) of constant-pressure MD were carried out at 300 K. All of the  $\alpha$  carbons were blocked with a harmonic force constant of 10 kcal/mol·Å. The final structure of the complexes was obtained as the average of the last 400 ps (700 ps for the ER $\alpha$  and ER $\beta$  complexed with estradiol) of MD minimized with the CG method until a convergence of 0.05 kcal/mol·Å.

For the ligands, the force fields parameters were taken from the general Amber force field (GAFF), whereas the atomic partial charges were derived by semiempirical AM1 geometry optimization and subsequent single point Hartree–Fock (HF)/6-31G\* calculation of the electrostatic potential, to which the charges were fitted using the RESP procedure.<sup>40</sup>

To verify whether using these parameters the ligands were able to maintain the intramolecular H bond and consequently the pseudocycle, the simulation protocol applied to the receptor–ligand complex as described above was applied to compound **2b** immersed in an explicit solvent model TIP3P water with a 20 Å water cap. The minimized average of the last 400 ps of MD showed the presence of the intramolecular H bond and the pseudocycle; furthermore, the superimposition of this structure with the one optimized with the QM method (conformation **a** of Table 5) showed a value of 0.40 of RMSD (evaluated on all the atoms).

**Energy Evaluation.** We extracted 200 snapshots (at time intervals of 2 ps) for each species (complex, receptor and ligand) from the last 400 ps of MD of the 44 ligand–ER complexes. The various MM-PBSA energy terms in eq 1 were computed as follows:

$$G = G_{\text{polar}} + G_{\text{nonpolar}} + E_{\text{mm}} - TS \quad (1)$$

Electrostatic, van der Waals, and internal energies ( $E_{\text{mm}}$ ) were obtained using the SANDER module in AMBER 8.0.<sup>39</sup> Polar energies ( $G_{\text{polar}}$ ) were obtained from the PBSA module of AMBER 8.0 program (using the Poisson–Boltzmann method), applying dielectric constants of 1 and 80 to represent gas and water phases, respectively. Nonpolar energies ( $G_{\text{nonpolar}}$ ) were determined using the MOLSURF program.

To compare the energetic interactions of the two orientations (A and B in Figure 3) of the same ligand into the same receptor, we took into account only the first three terms of eq 1, considering the entropic value to be approximately constant.

$$\Delta G_{\text{bind}} = G_{\text{complex}} - (G_{\text{protein}} + G_{\text{ligand}}) \quad (2)$$

Solute entropy was evaluate only for the best orientation of each ligand into the two receptors to correlate the predicted free energy of binding (calculated as in eq 2) with the experimental one. It was estimated using the NMODE module of AMBER 8.0 on a total of 10 snapshots. Prior to the normal mode calculations, each species (complex, receptor, or ligand) was subjected to a CG energy minimization using a distance dependent dielectric, until a convergence of 0.00001 kcal/mol·Å.

**Acknowledgment.** We are grateful for the financial support provided by grants from the National Institutes of Health (R37 DK15556, R37 CA25836, and P01AG024387 to J.A.K.).

**Supporting Information Available:** Tables reporting the combustion analysis data and the MM-PBSA results calculated for each ligand (A and B conformations) in both receptor subtypes

(ER $\alpha$  and ER $\beta$ ). This material is available free of charge via the Internet at <http://pubs.acs.org>.

## References

- Katzenellenbogen, J. A.; Katzenellenbogen, B. S. Nuclear hormone receptors: ligand-activated regulators of transcription and diverse cell responses. *Chem. Biol.* **1996**, *3*, 529–536.
- Kuiper, G. G. J. M.; Enmark, E.; Peltö-Huikko, M.; Nilsson, S.; Gustafsson, J.-A. Cloning of a novel receptor expressed in rat prostate and ovary. *Proc. Natl. Acad. Sci. U.S.A.* **1996**, *93*, 5925–5930.
- Kuiper, G. G. J. M.; Carlsson, B.; Grandien, K.; Enmark, E.; Haggblad, J.; Nilsson, S.; Gustafsson, J.-A. Comparison of the ligand binding specificity and transcript tissue distribution of estrogen receptors alpha and beta. *Endocrinology* **1997**, *138*, 863–870.
- Mosselman, S.; Polman, J.; Dijkema, R. ER $\beta$ : Identification and characterization of a novel human estrogen receptor. *FEBS Lett.* **1996**, *392*, 49–53.
- Pike, A. C. W.; Brzozowski, A. M.; Hubbard, R. E.; Bonn, T.; Thorsell, A. G.; Engstrom, O.; Ljunggren, J.; Gustafsson, J.-A.; Carlquist, M. Structure of the ligand-binding domain of oestrogen receptor beta in the presence of a partial agonist and a full antagonist. *EMBO J.* **1999**, *18*, 4608–4618.
- Brzozowski, A. M.; Pike, A. C. W.; Dauter, Z.; Hubbard, R. E.; Bonn, T.; Engström, O.; Öhman, L.; Greene, G. L.; Gustafsson, J.-A.; Carlquist, M. Molecular basis of agonism and antagonism in the oestrogen receptor. *Nature* **1997**, *389*, 753–758.
- Weihua, Z.; Andersson, S.; Cheng, G.; Simpson, E. R.; Warner, M.; Gustafsson, J.-A. Update on estrogen signaling. *FEBS Lett.* **2003**, *546*, 17–24.
- Katzenellenbogen, B. S.; Katzenellenbogen, J. K. Defining the <<S>> in SERMs. *Science* **2002**, *295*, 2380–2381.
- Grese, T. A.; Dodge, J. A. Selective estrogen receptor modulators (SERMs). *Curr. Pharm. Des.* **1998**, *4*, 71–92.
- Lin, X.; Huebner, V. Non-steroidal ligands for steroid hormone receptors. *Curr. Opin. Drug Discovery Dev.* **2000**, *3*, 383–398.
- Katzenellenbogen, J. A.; O'Malley, B. W.; Katzenellenbogen, B. S. Tripartite steroid hormone receptor pharmacology: Interaction with multiple effector sites as a basis for the cell- and promoter-specific action of these hormones. *Mol. Endocrinol.* **1996**, *10*, 119–131.
- McKenna, N. J.; O'Malley, B. W. Combinatorial control of gene expression by nuclear receptors and coregulators. *Cell* **2002**, *108*, 465–474.
- Minutolo, F.; Bertini, S.; Papi, C.; Carlson, K. E.; Katzenellenbogen, J. A.; Macchia, M. Salicylaldoxime moiety as a phenolic "A-ring" substitute in estrogen receptor ligands. *J. Med. Chem.* **2001**, *44*, 4288–4291.
- Minutolo, F.; Antonello, M.; Bertini, S.; Rapposelli, S.; Rossello, A.; Sheng, S.; Carlson, K. E.; Katzenellenbogen, J. A.; Macchia, M. Synthesis, binding affinity, and transcriptional activity of hydroxy- and methoxy-substituted 3,4-diarylsalicylaldoximes on estrogen receptors  $\alpha$  and  $\beta$ . *Bioorg. Med. Chem.* **2003**, *11*, 1247–1257.
- Anstead, G. M.; Carlson, K. E.; Katzenellenbogen, J. A. The estradiol pharmacophore: ligand structure-estrogen receptor binding affinity relationships and a model for the receptor binding site. *Steroids* **1997**, *62*, 268–303.
- Minutolo, F.; Antonello, M.; Bertini, S.; Ortore, G.; Placanic, G.; Rapposelli, S.; Sheng, S.; Carlson, K. E.; Katzenellenbogen, B. S.; Katzenellenbogen, J. A.; Macchia, M. Novel estrogen receptor ligands based on an anthranilyldoxime structure: Role of the phenol-type pseudocycle in the binding process. *J. Med. Chem.* **2003**, *46*, 4032–4042.
- Kollman, P. A.; Massova, I.; Reyes, C.; Kuhn, B.; Huo, S.; Chong, L.; Lee, M.; Lee, T.; Duan, Y.; Wang, W.; Donini, O.; Cieplak, P.; Srinivasan, J.; Case, D. A.; Cheatham, T. E. 3rd Calculating structures and free energies of complex molecules: combining molecular mechanics and continuum models. *Acc. Chem. Res.* **2000**, *33*, 889–897.
- Miyaura, N.; Suzuki, A. Palladium-catalyzed cross-coupling reactions of organoboron compounds. *Chem. Rev.* **1995**, *95*, 2457–2483.
- Littke, A. F.; Fu, G. C. A convenient and general method for Pd-catalyzed Suzuki cross-couplings of aryl chlorides and arylboronic acids. *Angew. Chem., Int. Ed.* **1998**, *37*, 3387–3388.
- Lamm, B.; Liedholm, B. Nucleophilic aromatic substitution reactions. III. Replacement of bromine by chloride ion in 2-bromo-3-nitro- and 2-bromo-5-methyl-3-nitrobenzenediazonium ions. *Acta Chem. Scand.* **1967**, *21*, 2679–2688.
- Karabatsos, G. J.; Hsi, N. Structural studies by nuclear magnetic resonance-XI: Conformations and configurations of oxime O-methyl ethers. *Tetrahedron* **1967**, *23*, 1079–1095.
- Katzenellenbogen, J. A.; Johnson, H. J., Jr.; Myers, H. N. Photo-affinity labels for estrogen binding proteins of rat uterus. *Biochemistry* **1973**, *12*, 4085–4092.

- (23) Carlson, K. E.; Choi, I.; Gee, A.; Katzenellenbogen, B. S.; Katzenellenbogen, J. A. Altered ligand binding properties and enhanced stability of a constitutively active estrogen receptor: Evidence that an open-pocket conformation is required for ligand interaction. *Biochemistry* **1997**, *36*, 14897–14905.
- (24) Eiler, S.; Gangloff, M.; Duclaud, S.; Moras, D.; Ruff, M. Overexpression, purification, and crystal structure of native ER alpha LBD. *Protein Expression Purif.* **2001**, *22*, 165–173.
- (25) Manas, E. S.; Xu, Z. B.; Unwalla, R. J.; Somers, W. S. Understanding the selectivity of genistein for human estrogen receptor-beta using X-ray crystallography and computational methods. *Structure* **2004**, *12*, 2197–2207.
- (26) Brzozowski, A. M.; Pike, A. C.; Dauter, Z.; Hubbard, R. E.; Bonn, T.; Engstrom, O.; Ohman, L.; Greene, G. L.; Gustafsson, J. A.; Carlquist, M. Molecular basis of agonism and antagonism in the oestrogen receptor. *Nature* **1997**, *389*, 753–758.
- (27) Pike, A. C.; Brzozowski, A. M.; Hubbard, R. E.; Bonn, T.; Thorsell, A. G.; Engstrom, O.; Ljunggren, J.; Gustafsson, J. A.; Carlquist, M. Structure of the ligand-binding domain of oestrogen receptor beta in the presence of a partial agonist and a full antagonist. *EMBO J.* **1999**, *18*, 4608–4618.
- (28) Morris, G. M.; Goodsell, D. S.; Halliday, R. S.; Huey, R.; Hart, W. E.; Belew, R. K.; Olson, A. J. Automated docking using a Lamarckian genetic algorithm and empirical binding free energy function. *J. Comput. Chem.* **1998**, *19*, 1639–1662.
- (29) Mewshaw, R. E.; Edsall, R. J., Jr.; Yang, C.; Manas, E. S.; Xu, Z. B.; Henderson, R. A.; Keith, J. C., Jr.; Harris, H. A. ERbeta ligands. 3. Exploiting two binding orientations of the 2-phenyl-naphthalene scaffold to achieve ERbeta selectivity. *J. Med. Chem.* **2005**, *48*, 3953–3979.
- (30) Yang, C.; Edsall, R., Jr.; Harris, H. A.; Zhang, X.; Manas, E. S.; Mewshaw, R. E. ERβ Ligands. Part 2: Synthesis and structure–activity relationships of a series of 4-hydroxy-biphenyl-carbaldehyde oxime derivatives. *Bioorg. Med. Chem.* **2004**, *12*, 2553–2570.
- (31) Kuhn, B.; Kollman, P. A. Binding of a diverse set of ligands to avidin and streptavidin: an accurate quantitative prediction of their relative affinities by a combination of molecular mechanics and continuum solvent models. *J. Med. Chem.* **2000**, *43*, 3786–3791.
- (32) Donini, O. A.; Kollman, P. A. Calculation and prediction of binding free energies for the matrix metalloproteinases. *J. Med. Chem.* **2000**, *43*, 4180–4188.
- (33) Huo, S.; Wang, J.; Cieplak, P.; Kollman, P. A.; Kuntz, I. D. Molecular dynamics and free energy analyses of cathepsin D–inhibitor interactions: Insight into structure-based ligand design. *J. Med. Chem.* **2002**, *45*, 1412–1419.
- (34) Wrenn, C. K.; Katzenellenbogen, B. S. Structure–function analysis of the hormone binding domain of the human estrogen receptor by region-specific mutagenesis and phenotypic screening in yeast. *J. Biol. Chem.* **1993**, *268*, 24089–24098.
- (35) McInerney, E. M.; Weis, K. E.; Sun, J.; Mosselman, S.; Katzenellenbogen, B. S. Transcription activation by the human estrogen receptor subtype β (ERβ) studied with ERβ and ERα receptor chimeras. *Endocrinology* **1998**, *139*, 4513–4522.
- (36) Berman, H. M.; Westbrook, J.; Feng, Z.; Gilliland, G.; Bhat, T. N.; Weissig, H.; Shindyalov, I. N.; Bourne, P. E. The Protein Data Bank. *Nucl. Acids Res.* **2000**, *28*, 235–242.
- (37) *Macromodel*, version 8.5; Schrodinger Inc., Portland, OR, 1999.
- (38) <http://www.scripps.edu/~sanner/python/adt>.
- (39) Case, D. A.; Darden, T. A.; Cheatham, T. E., III; Simmerling, C. L.; Wang, J.; Duke, R. E.; Luo, R.; Merz, K. M.; Wang, B.; Pearlman, D. A.; Crowley, M.; Brozell, S.; Tsui, V.; Gohlke, H.; Mongan, J.; Hornak, V.; Cui, G.; Beroza, P.; Schafmeister, C.; Caldwell, J. W.; Ross, W. S.; Kollman, P. A. *AMBER 8*; University of California: San Francisco, CA, 2004.
- (40) Bayly, C. I.; Cieplak, P.; Cornell, W. D.; Kollman, P. A. A well-behaved electrostatic potential based method using charge restraints for determining atom-centered charges: The RESP model. *J. Phys. Chem.* **1993**, *97*, 10269–10280.

JM060560U